

Winter performance of a Solar Humidification Dehumidification Desalination System

Reza Enayatollahi

Submitted to the
Institute of Graduate Studies and Research
in partial fulfillment of the requirements for the Degree of

Master of Science
in
Mechanical Engineering

Eastern Mediterranean University
January 2012
Gazimağusa, North Cyprus

Approval of the Institute of Graduate Studies and Research

Prof. Dr. Elvan Yılmaz
Director

I certify that this thesis satisfies the requirements as a thesis for the degree of Master of Science in Mechanical Engineering.

Assoc. Prof. Dr. Uğur Atikol
Chair, Department of Mechanical Engineering

We certify that we have read this thesis and that in our opinion it is fully adequate in scope and quality as a thesis for the degree of Master of Science in Mechanical Engineering.

Assoc. Prof. Dr. Uğur Atikol
Supervisor

Examining Committee

1. Assoc. Prof. Dr. Fuat Egeliolu

2. Assoc. Prof. Dr. Uğur Atikol

3. Assist. Prof. Dr. Hasan Hacışevki

ABSTRACT

The present study is concerned with desalinating the saline water, using the humidification dehumidification method. An open air open water cycle is chosen, whilst forced air circulation is applied. The system utilizes water and air heating technique. The energy required for heating the air is provided by solar radiation, while the required energy for heating the water is provided by electricity. The goals of this study are:

- a) To study different existing systems in the literature
- b) To review the governing equations for each segment of the desalination unit
- c) To conduct an experiment on the above described humidification dehumidification desalination unit under North Cyprus winter conditions

The solar air heater placed to azimuth angle of -20° , with a tilt angle of 45° . According to the experiment, the optimum flow rate for water stream is 4 Lt/min, while the air flow rate is $1.5 \text{ m}^3/\text{min}$. Besides, the inlet water temperature to the evaporator is kept at 55°C . The maximum productivity of 1.55 Lt/day.m^2 is achieved for this condition. The present experiment implies that the maximum productivity is achieved with higher temperature of both air and water streams into the evaporator, higher flow rate for water and lower flow rate for air.

Keywords: Humidification, Dehumidification, Desalination

ÖZ

Bu çalışma nemlendirme ve nem alma methodu kullanılarak tuzlu suyu tuzdan arındırmayı kapsamaktadır. Bir açık hava, açık su devresi seçilerek fanlı sirkülasyon uygulanmıştır. Bu sistem su ve hava ısıtma tekniğinden faydalanmaktadır. Havayı ısıtmak için gerekli enerji güneş radyasyonu tarafından karşılanırken suyu ısıtmak için elektrik enerjisi kullanılmıştır. Çalışmanın Amacı:

- a) Bu konuda yapılmış önceki çalışmaları incelemek
- b) Tuzdan arındırma ünitesinin her aşamasında mevcut denklemleri yeniden gözden geçirmek
- c) Kuzey Kıbrıs kış hava şartlarında; nemlendirme ve nem alma yöntemiyle yukarıda bahsi geçen tuzdan arındırma ünitesini deneye tabi tutmak

Güneşli hava toplayıcısı güneyden doğuya doğru 20°'lik açıyla yerleştirilmiş olup yataydan 45° lik eğimle monte edilmiştir. Deneye göre su buharının ideal akış hızı 4 lt/dk iken; hava akış hızı 1.5m³/dk'dır. Ayrıca; suyun buharlaştırıcıya giriş sıcaklığı 55°C'de tutulmuştur. Maksimum üretim 1.55 Lt/gün.m² olarak gerçekleştirilmiştir. Bu çalışmada azami su üretiminin sağlanabilmesi için su ve havanın daha yüksek sıcaklıklarda olmasının, su debisinin artırılmasının ve hava debisinin azaltılmasının gerektiği ortaya çıkmıştır.

Anahtar Kelimeler: Nemlendirme, Nem alma, Tuzdan Arındırma

Dedicated to
My Beloved Family

ACKNOWLEDGMENTS

I take this opportunity to be grateful to my supervisor and the chairman of department, Assoc. Prof. Dr. Ugur Atikol for guiding me all along my thesis research and experiment. Without his priceless supervision, it would be impossible to finish this thesis.

I would like to thank, sincerely to my friend Maher T.S.Ghazal who kindly shared his knowledge and experiences with me.

Also, I appreciate the efforts of my dear friends which they have supported me in my thesis. Although, I did not mention their names; however, they will remain in my heart forever.

Last but not least, I would like to express my deepest appreciation to my family who allowed me to travel to Cyprus and supported me during my education.

TABLE OF CONTENTS

ABSTRACT.....	iii
ÖZ.....	iv
DEDICATION.....	iv
ACKNOWLEDGMENTS.....	vi
LIST OF TABLES.....	ix
LIST OF FIGURES.....	x
LIST OF ABBREVIATIONS.....	xiii
NOMENCLATURE.....	xiv
1. INTRODUCTION.....	1
1.1 Motivation.....	1
1.2 Scope and Objectives.....	2
2. LITERATURE REVIEW.....	4
2.1 HDH Desalination.....	4
2.2 Classifications.....	5
2.3 Historical Review.....	6
3. REVISION OF THE GOVERNING EQUATIONS.....	22
3.1 Introduction.....	22
3.2 Solar Air Collector.....	23
3.2.1 Energy Balance.....	24
3.2.2 Absorbed Solar Radiation.....	27
3.2.3 Humidity Calculation.....	28
3.3 Evaporator.....	30
3.4 Condenser.....	35

4. EXPERIMENTAL SETUP	41
4.1 System Description	41
4.2 Uncertainty analysis.....	48
5. RESULTS AND DISCUSSION	49
6. CONCLUSIONS AND FUTURE WORK	75
6.1 Conclusions.....	75
6.2 Future Work.....	76
REFERENCES	77
APPENDIX.....	80

LIST OF TABLES

Table 2-1: Summary of the Cost of Different Solar Base HDH Units.	19
Table 5-1: The Temperatures of Air and Water Streams at Operating Conditions on December 21 th	50
Table 5-2: The Measured Values for December 27 th	51
Table 5-3: The Measured Values for December 28 th	54
Table 5-4: Measured Values of December 29 th	57
Table 5-5: Measured Values of January 4 th	60
Table 5-6: Measured Values of January 5 th	63
Table 5-7: Observed Values of the Experiment on January 6 th	66
Table 5-8: Observed Values of the January 7 th	69
Table 5-9: The Measured Values on January 8 th	72

LIST OF FIGURES

Figure 2-1: Rains Cycle.	5
Figure 2-2: HDH Desalination Classifications.	6
Figure 2-3: Multi-Effect CAOW Water-Heated System.	7
Figure 2-4: a. Schematic of the Proposed Desalination Process. b. Photo of the Experimental Unit.	9
Figure 2-5: Sketch of the Desalination System.	10
Figure 2-6: A Schematic Diagram of the Solar Desalination System.	12
Figure 2-7: a) CAOW-AH, b) OAOW-AH, c) CAOW-WH, d) OAOW-WH	14
Figure 2-8: Sketch of the HDH Desalination Unit with Closed Air Cycle and Water Heating Technique.	15
Figure 2-9: Sketch of a Natural Draft Air Circulation MEH Desalination System. ...	16
Figure 2-10: Schematic of a Desalination Unit with Air and Water Heating and Closed Water Cycle.	17
Figure 2-11: Sketch of a Water Heating Closed Air Cycle Desalination Unit.	18
Figure 2-12: A Schematic of Experimental Unit.	20
Figure 2-13: A Solar Base HDH Desalination System.	21
Figure 3-1: Desalination Unit	23
Figure 3-2: Solar Air Collector	24
Figure 3-3: Cascading Evaporator	30
Figure 3-4: Fined Condenser	36
Figure 4-1: HDH Desalination Unit	41
Figure 4-2: Pyranometer	43
Figure 4-3: Water Flow Meter	43

Figure 4-4: Air Flow Meter (Anemometer)	44
Figure 4-5: Digital Thermometer	44
Figure 4-6: Fan.....	45
Figure 4-7: Air Collector	45
Figure 4-8: Condenser.....	46
Figure 4-9: Evaporator	46
Figure 4-10: Water Heater	47
Figure 5-1: Insolation on the Collector Surface during December 21 st	49
Figure 5-2: Total Radiation on December 27 th	52
Figure 5-3: Water Production versus Time on December 27 th	52
Figure 5-4: Water Production versus Total Rate of Energy Gained On December 27 th , (Total Energy = Solar Energy + Electrical Energy)	53
Figure 5-5: Variation of Insolation during the Day of December 28 th	55
Figure 5-6: Variation of Water Production during the Day of December 28 th	55
Figure 5-7: Water Production versus Total Rate of Energy Gained On December 28 th , (Total Energy = Solar Energy + Electrical Energy)	56
Figure 5-8: Variation of Irradiance during December 29 th	58
Figure 5-9: Hourly Water Production on December 29 th	58
Figure 5-10: Water Production versus Total Rate of Energy Gained On December 29 th , (Total Energy = Solar Energy + Electrical Energy)	59
Figure 5-11: Hourly Variation of Irradiance during January 4 th	61
Figure 5-12: Hourly Production of Water during January 4 th	61
Figure 5-13: Water Production versus Total Rate of Energy Gained On January 4 th , (Total Energy = Solar Energy + Electrical Energy).....	62
Figure 5-14: Hourly Variation of Insolation on January 5 th	64

Figure 5-15: Hourly Water Production during the Day of January 5 th	64
Figure 5-16: Water Production versus Total Rate of Energy Gained On January 5 th , (Total Energy = Solar Energy + Electrical Energy).....	65
Figure 5-17: Variation of Irradiance during the January 6 th	67
Figure 5-18: Hourly Production of Water during January 6 th	67
Figure 5-19: Water Production versus Total Rate of Energy Gained On January 6 th , (Total Energy = Solar Energy + Electrical Energy).....	68
Figure 5-20: Variation of Insolation on January 7 th	70
Figure 5-21: Hourly Changing the Water Production on January 7 th	70
Figure 5-22: Water Production versus Total Rate of Energy Gained On January 7 th , (Total Energy = Solar Energy + Electrical Energy).....	71
Figure 5-23: Hourly Changing Of Irradiance on January 8 th	73
Figure 5-24: Hourly Changing Of Water Production during January 8 th	73
Figure 5-25: Water Production versus Total Rate of Energy Gained On January 8 th , (Total Energy = Solar Energy + Electrical Energy).....	74
Figure A-1: psychometric chart	81

LIST OF ABBREVIATIONS

AH	Air Heated
AWH	Air and Water Heated
CAOW	Closed Air Open Water
DOE	Design Of Experiment method
HDH	Humidification Dehumidification
MED	Multi Effect Desalination
MEH	Multi Effect Humidification
MSF	Multi Stage Flash
MVC	Mechanical Vapor Compression
OAOW	Open Air Open Water
RO	Reverse Osmosis
TTD	Terminal Temperature Difference
TVC	Thermally Vapor Compression
VC	Vapor Compression
W	Watt
WH	Water Heated

NOMENCLATURE

A	Area
A_s	specific area
C_p	specific heat
C_v	concentration of vapor in the air
D	mass diffusion coefficient
D_p	pipe diameter
F'	collector efficiency factor
F_R	collector heat removal factor
h	convection heat transfer coefficient
h_A	enthalpy of air
h_w	enthalpy of water
h_v	enthalpy of water vapor
H	total radiation on a horizontal surface
H_a	absorbed radiation
H_B	beam radiation on a horizontal surface
H_d	diffuse radiation on a horizontal surface
H_t	total radiation
K	thermal conductivity
m_a	mass of dry air
m_g	maximum mass of moisture in the air
m_v	mass of moisture in the air
\dot{m}	mass flow rate
P_g	saturation pressure of water

P_v	partial pressure of water vapor
$P_{s@T}$	saturation pressure at the specific temperature of T
Q_u	useful energy gain
R	thermal resistance
R_B	the beam radiation tilted factor
R_v	universal gas constant
Re	Reynolds number
s	tilted angle
T	temperature
u	velocity
U	overall heat transfer coefficient
U_c	collector overall heat loss coefficient
V	volume
\dot{V}	volumetric flow rate

Greek symbols

α	absorptivity
η	efficiency
μ	dynamic viscosity
ρ	density
ρ_g	ground reflectivity
τ	transmissivity
$\tau\alpha$	transmissivity-absorptivity product
ϕ	relative humidity
ω	specific humidity

subscripts

a	ambient
A	air
B	beam
c	collector
d	diffuse
f	fin
g	ground
in	inlet
out	outlet
w	water
v	water vapor

Chapter 1

INTRODUCTION

1.1 Motivation

Three quarter of the earth's surface is covered with water, but only 3% of this water is potable water [1], which human beings and animals are able drink. Shortage of potable water strongly motivated scientists to find a solution for converting brackish water to desalinated water.

The humidification-dehumidification (HDH) desalination technique is a low temperature procedure to provide small amount of potable water [2]. It consumes lower amount of energy than the other methods of desalination. Furthermore, in this process, coolant is the saline water and heating fluid is the moist air. It is common practice to use ammonia or other refrigerants as coolant. Using such working fluids needs additional components such as compressors and expansion devices which may consume energy. Besides, in case of any leakage they may contaminate the produced water. since in HDH desalination systems the cooling fluid is saline water that requires no extra energy consuming devices, the process is simpler and there is no danger of contamination of the produced fresh water.

Typical desalination units are producing potable water, but most of them are burning fossil fuels, directly or indirectly to provide the required energy for heating sea water [3]. Burning fossil fuels has several undesirable impacts on the environment such as;

polluting the air with toxic gases and increasing the quantity of green house gases in the atmosphere. Moreover, the fossil fuels themselves are quite expensive; furthermore, the amount of fossil fuels on earth is finite. Therefore, using the renewable and clean sources of energy is strongly suggested to prevent such drawbacks.

The present study is performed in North Cyprus, which has approximately 300 sunny days per year, and suffers from the shortage of potable water. Hence, producing potable water from saline water by using the solar energy as the source of heat is the objective of the study.

1.2 Scope and Objectives

The present work is concerned with the setting up and conduction of an experiment on a HDH desalination system designed by Kraft et al. [4] to find its suitability for the North Cyprus winter conditions.

A review study, on the researches and experiments carried out before, is essential to find out the most up to date and effective desalination units. By a review study, one may be able to find a proper system for the location of study, according to availability of the requirements in there.

A review of the governing equations may help understanding the thermodynamics of the system considered. This may also help the student who seek to carry out theoretical analysis.

The inlet and outlet temperature difference of the moist air in the condenser, and the condenser inlet humidity of the air are the most important parameters affecting the potable water production. These parameters change with changing flow rates of both water and air streams. Besides, the temperature of both water and air streams are influential on the production. Therefore, optimizing the flow rates for both water and air flows, in addition to evaluate the impact of changing the water temperature, are aimed for the current experiment.

In Chapter 2, the previous experiments and researches on the HDH desalination unit, which they are most relevant to the current experiment, are reviewed and explained very briefly.

In Chapter 3, the governing equations for each segment of the HDH desalination system are discussed theoretically.

Moreover, Chapter 4 discusses the configuration, and the procedure of HDH desalination unit under the study is explained.

Furthermore, chapter 5 presents the results of the experiment, in detail.

Besides, in Chapter 6 the results of the experiment is discussed and the suggestions are presented.

Chapter 2

LITERATURE REVIEW

2.1 HDH Desalination

Solar humidification-dehumidification desalination technique is said to be a low temperature procedure for producing a small amount of potable water [4]. This technique presents several advantages such as; flexibility in capacity, moderate installation, operating expenses, simplicity, and the possibility of using low temperature energy sources. Furthermore, HDH units have the capability of working with renewable energy sources like solar energy, which is accessible in barren regions and isolated islands. The best application of HDH desalination systems is to provide the drinking water for a family house.

The philosophy behind the HDH desalination method is the natural rain cycle [5]. In the natural rain cycle water evaporates from the oceans by the sun. The water vapor moisturizes the surrounding air, the humid air then rises to high levels of atmosphere, and because of low temperature there, water will be condense and form the rain drops. Rain drops return to the earth and can be used as drinking water. A diagram of this cycle is indicated in Figure 2.1.

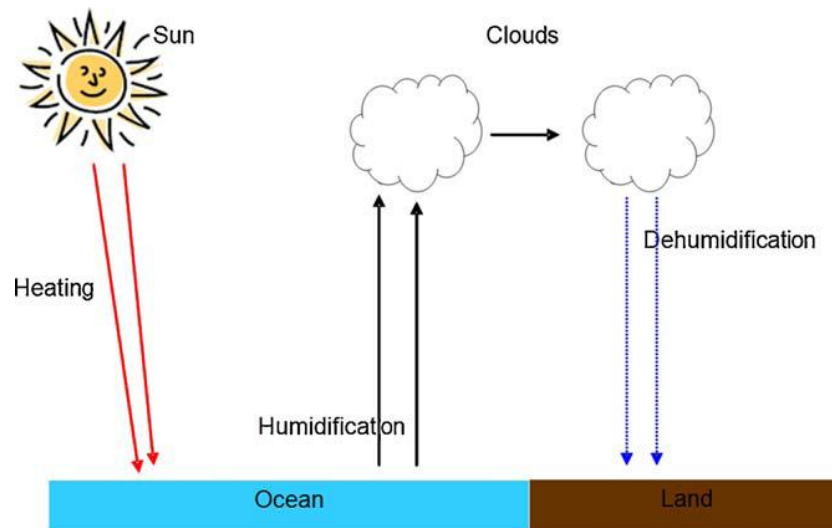


Figure 2-1: Rains Cycle [5].

A similar procedure is conducting in a typical, manmade, HDH unit. Almost all of humidification dehumidification desalination structures, have three segments; a heater, an evaporator and a condenser. Depends on the heating technique applied for the experiment the heater can be water or air heated system, or a grouping of them both. Depends on the accessibility of different source of energies, the heating source might be; solar, geothermal, electric heaters or even burning the fossil fuels directly. Variety of evaporator and condenser can be used, depends on the effectiveness and area, necessary for the system.

2.2 Classifications

As it mentioned earlier, the heating procedure for the humidification can be water or air heating, or a combination of them. Therefore, in this way HDH desalination systems can be categorize in three groups; water heated, air heated and water and air heated systems.

Another way to classify HDH system is based on the cycle they are using for both streams, whether it is an open or closed cycle [5]. Therefore, they have been

classified in four groups; open air-open water, open air- closed water, closed air- open water and closed air-closed water.

Furthermore, desalination system can be classified by the method using for air circulation in two categories; forced and natural circulation.

Combination of these three methods of classification yields the diagram illustrated in Figure 2.2.

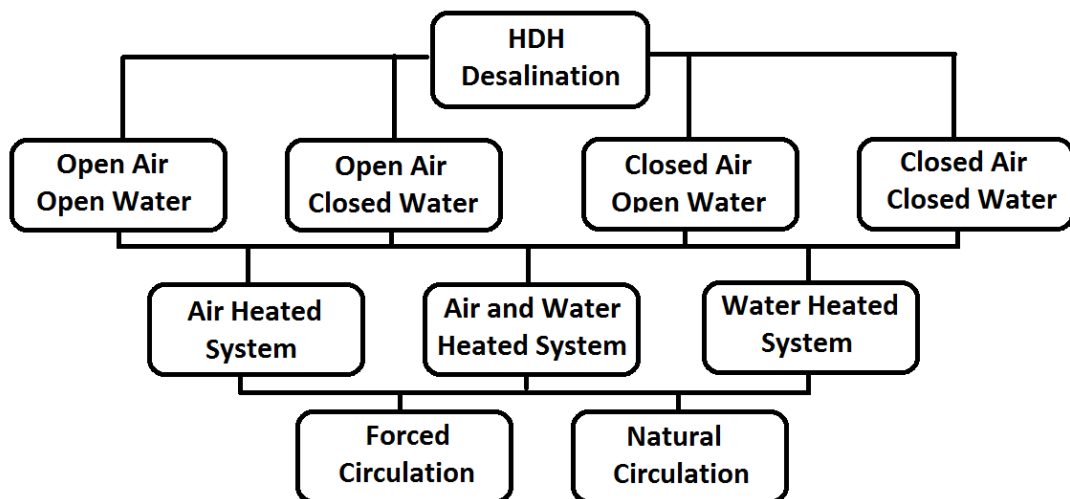


Figure 2-2: HDH Desalination Classifications.

2.3 Historical Review

There are extensive numbers of experiments, researches and papers on humidification dehumidification desalination process from different aspects. I will mention some of them in following which they are most relevant to my work, and I have used them in my thesis.

Prakash Narayan, Mostafa H. Sharqawy, Edward K. Summers, John H. Lienhard, Syed M. Zubair, M.A. Antar, in “2009”, [5], reviewed different methods of desalination. They compared them with humidification dehumidification units driven by solar energy, ether solar water heating or solar air heating systems. They have mentioned two main process of desalination as: by evaporation or by using a semi-permeable membrane to extract fresh water from saline water. Besides, they have introduced multistage flash (MSF), multiple effect desalination (MED) and vapor compression (VC), either thermally (TVC) or mechanically (MVC), as the most valuable commercial desalination processes. On the other hand, they have classified desalination units under three categories; first, from the energy point of view; the energy used can be solar, thermal, geothermal or a hybrid system. Second, based on the cycle configuration; means closed or open cycle for air and water. Third, based on the heating procedure: water or air heating systems. In addition, they have reviewed the component design; solar air heaters, humidifiers and dehumidifiers. Finally, by a detailed review, they have found that, among all HDH systems, the multi-effect CAOW water-heated system is the most energy efficient. A schematic of this system is illustrated in Figure 2.3.

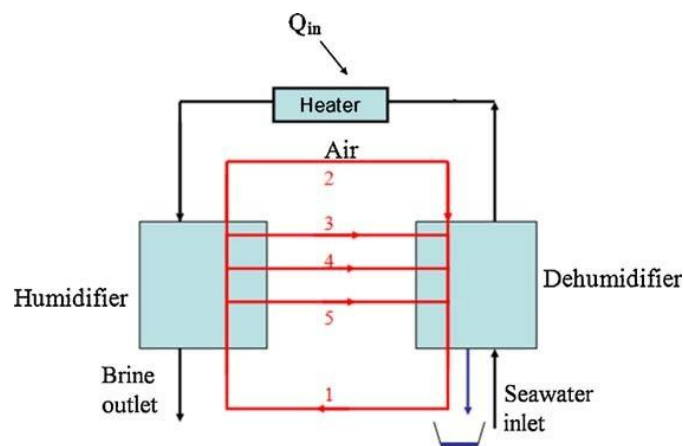


Figure 2-3: Multi-Effect CAOW Water-Heated System [5].

For this system, the cost of water production is 3 to 7 US\$ per meter cube. Even if this price is more than a same small scale RO system, the HDH systems have some other benefits for small scale decentralized water production. Such kinds of HDH units are easy to operate and maintenance, also they have much straightforward brine pre-treatment. Availability of requirements is another advantage of HDH desalination systems.

In “2010”, a study carried out by Veera Gnaneswar Gude, Nagamany Nirmalakhandan and Shuguang Deng, [6], objected to express the hypothetical rationale for a low temperature phase-change desalination process. In this procedure, saline water was evaporating at a temperature, about 15°C more than the ambient temperature. This process was under a near-vacuum pressure, created by the barometric head without any mechanical energy supply. The unit was including; two heat exchangers, an evaporation chamber, a natural draft condenser and three 10-m tall columns. An illustration of this system is indicated in Figure 2.4.

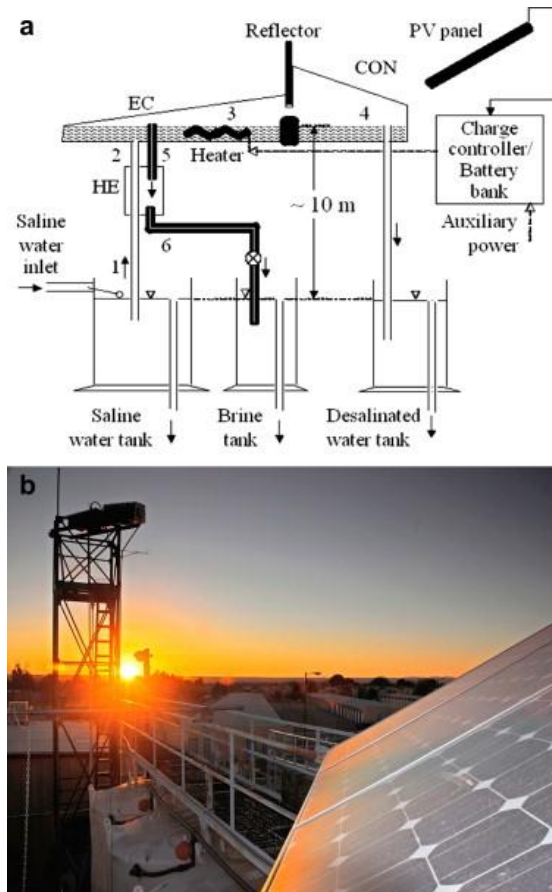


Figure 2-4: a. Schematic of the Proposed Desalination Process. b. Photo of the Experimental Unit [6].

These columns were serving as the brackish water column, the brine withdrawal column, and the potable water column. Increasing the saline water in the evaporation chamber was conducting the water vapor into the condenser. The condensate was drain into the fresh water column. The first heat exchanger was preheating the brackish water enters the evaporation chamber by the outlet brine stream from the evaporation chamber. Second heat exchanger proposed to provide the heat required to derive the process by a low grade heat source. It is fruitful to mention that; if the brackish and potable columns are keeping at the same temperature, the stream direction will be from saline column to the potable column.

In "2009" E.H.Amer, H. Kotb, G.H. Mostafa and El-Ghalban, [7], studied on a humidification dehumidification unit, theoretically and experimentally. Their HDH

installation contained two heat exchangers; one as a humidifier and the other one as a condenser or dehumidifier. They have used a heater which according to their report it could be a solar collector or any other heater. The system under their study had the dimensions of 1.2, 0.5, 2 meter, exclude the heat source, where it divided in two unequal parts via a partition. The unit was insulated from all sides by a 5 cm glass wool mates. Galvanized steel was used for the outer sides, while aluminum angles were formed the frame. In order to prevent leaking, silicon sealing was applied. A 20 Watt electric fan was supported at the top of dehumidifier to present the forced air circulation. A 0.5 Hp, center fugal pump was used to circulate water. The dimensions of the condensation tower were 200 cm height, 40 cm length, and 50 cm width. A copper tube was formed as a coil, where it was used as a condenser of 15 m length, and 1.27 centimeter outer diameter. Fins were applied in order to raise the surface area of the condenser. The entire surface area of the condenser coil and its fins was roughly 6 m². In Figure 2.5, a schematic of the above described unit is sketched.

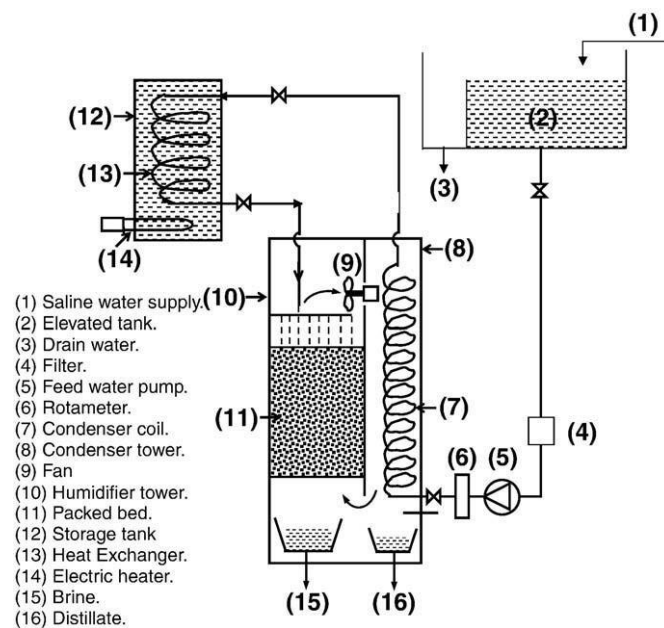


Figure 2-5: Sketch of the Desalination System [7].

The cooling water was flowed within the coil, and the air was flowed over the finned coil inside the condenser cabinet in a counter direction. The humidifier had the dimensions of; 200 cm height, 80 cm lengths, and 50 cm width. Inside the humidifier, a packing material was installed to provide a surface area of approximately 6 m². The packing was supported such that it did not block the air flow and remains continuously wet. The water was sprayed on the packing material using a hydraulic grid. A movable door was provided to facilitate the changing of packing material easily. Using the explained unit they had reached the maximum productivity of 5.41 L/h with wooden slates and about 5.81 L/h with forced air circulation. . The average deviation of theoretical prediction was 9% in the air temperature at condenser inlet, 3.8% in the humidity ratio at condenser exit and 1% in the water temperature at condenser exit.

In "2006" a theoretical study carried out by; J. Orfi, N. Galanis, M. Laplante, [8]. The study was objected to define the maximum production of distillated water with continuously adjust the ratio between the saline water and the air mass flow rates. The desalination under their study was consisting of two solar collectors; one for heating water and the other for air heating, besides an evaporator chamber and a condenser. Figure 2.6 is illustrating a schematic diagram of their system.

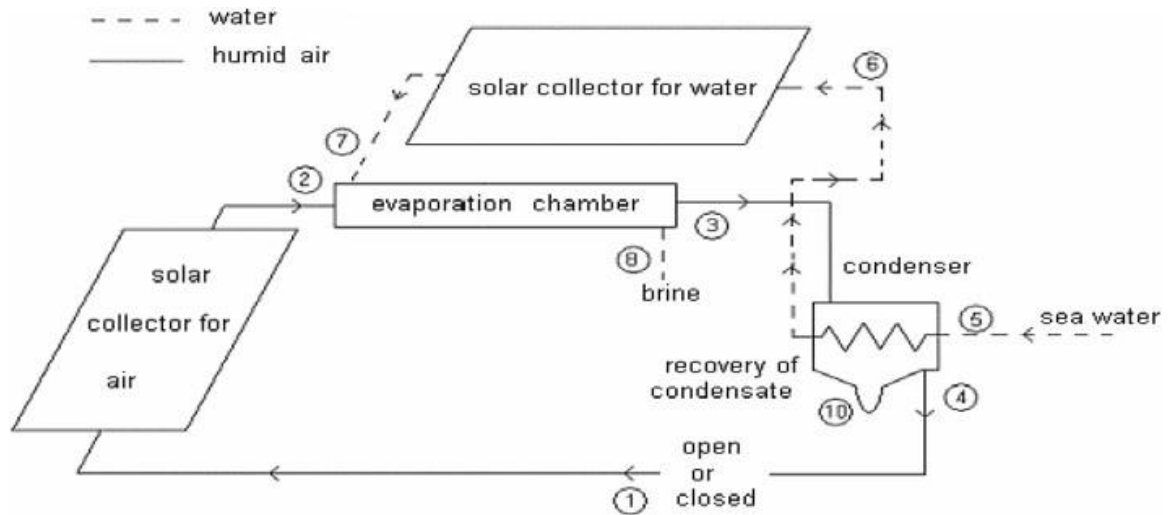


Figure 2-6: A Schematic Diagram of the Solar Desalination System [8].

Water and air were both heated in the collectors, and contact with each other in the evaporator chamber, in order to, moisturize the air. Heating water before it enters into the evaporator would reduce or eradicate the heat loss in the chamber, and consequently increases the outlet air temperature from the evaporator, and results in an increase in the amount of moisture carrying by air. Afterwards, in the condenser hot and moist air, in contact with sea water gets cold, and fresh water will extracted. Preheated seawater in the condenser then goes to the solar water collector. Based on the authors report; the air cycle can be either open or closed and the moist air can be humidified more than one time by returning back to the air collector. A mathematical modeling, based on mass and energy conservation, for each component of the desalination, was obtained. Accordingly it was found that the optimum mass flow rate of air is 0.05 kg/s, which it was leading the system to produce 5.6 L/hm². The corresponded optimal ratio of water to air mass flow rate was ranged between 0.88 and 1.96 for each month, whether for a closed or open system. It was observed for annual calculation that, for a constant mass flow rate of air, an open cycle can produce more potable water, than a closed system. It is fruitful to mention that all the

preceding data was obtained for an idealized situation for Monastir (35°N, 10°E), Tunisia.

Karan H. Mistry, Alexander Mitsos, John H. Lienhard V, [9], in "2010", worked on a humidification dehumidification desalination unit. The study was aimed to optimize HDH desalination cycle by applying nonlinear programming techniques. They have defined the governing equations for the humidifier and dehumidifier by approximating their both as adiabatic. The air and water heating systems was introduced to be single-stream heat exchangers. Applying the first and second law for the single-stream heat exchanger, results in obtaining the governing equations for water and air heating systems. Assumption of a constant heat flux, in addition to a greater temperature, for wall, than that of the bulk stream, was made for the heating systems. The analysis was conducted for closed air, open water and open air, open water HDH desalination cycles, each with air and water heating technique. These four systems are illustrated in Figure 2.7, a, b, c and d.

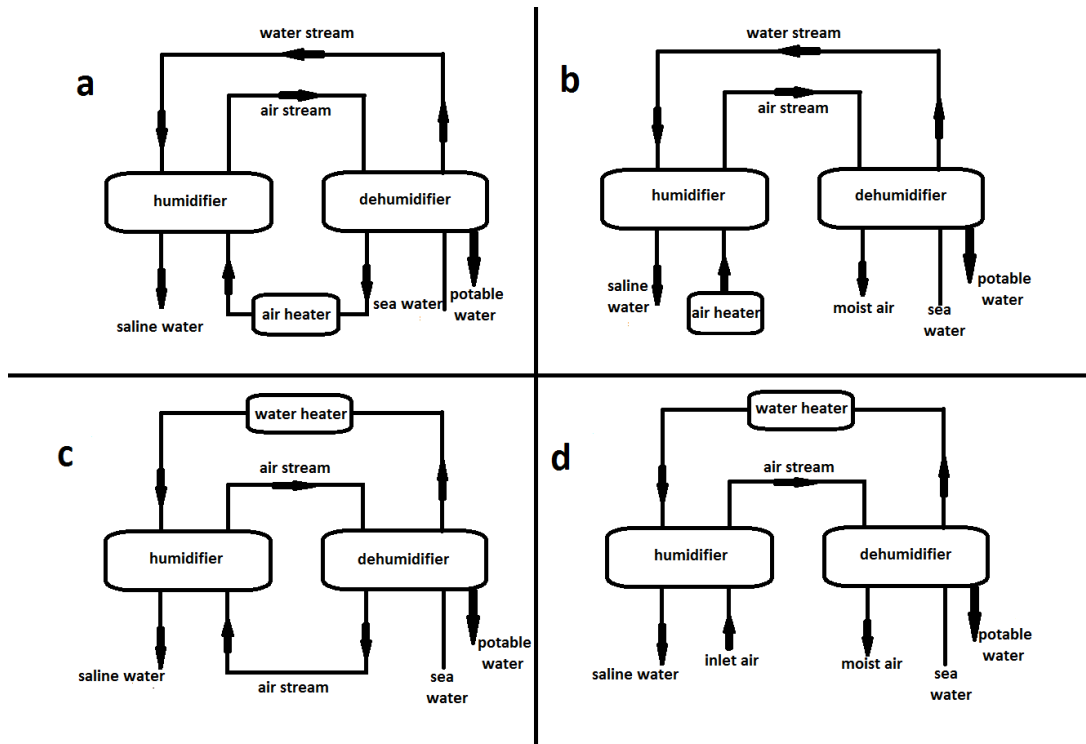


Figure 2-7: a) CAOW-AH, b) OAOW-AH, c) CAOW-WH, d) OAOW-WH

Based on the authors report; for a CAOW cycle with a terminal temperature difference (TTD) of 3°K , selecting the air heated system would result in higher performance. There is an inversely manner between TTD and the performance of both air and water heated systems. In the other hand, at low TTD air heated cycle defeats the water heated cycle, while, at higher TTD, an opposite would be correct. The authors also report that; the optimized OAOW-WH cycle always outperforms the optimized CAOW-WH cycle, but for the air heated cycle, CAOW cycle performs better than OAOW, except for the ambient relative humidity near 100%.

M. Mehrgoo, M. Amidpour, in “2010”, [10], designed and analyzed an HDH desalination unit by applying the concept of constructal theory. The constructal theory said to be about the methods of constructing systems that achieve their aims,

optimally. The main aim of the study was to maximize the potable water production. The system under the study was water heated, closed air cycle, HDH desalination unit. A schematic of the system is indicated in Figure 2.8.

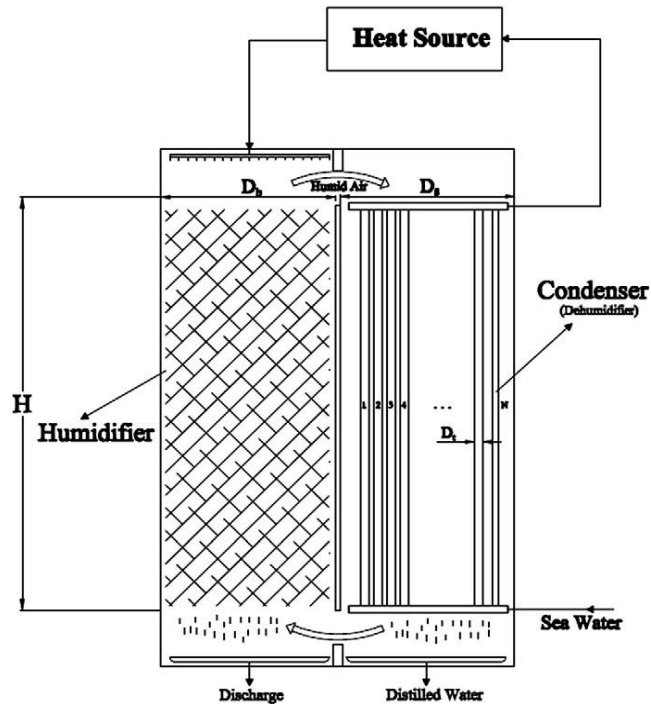


Figure 2-8: Sketch of the HDH Desalination Unit with Closed Air Cycle and Water Heating Technique [10].

After mathematical modeling for the unit, it was discovered that; the total volume, unit height and inlet temperature of cold and hot water are sensitive for designing HDH unit. The Effect of these three parameters was discussed, and the optimal values for each of them were reported.

M.M. Farid, Sandeep Parekh, J.R. Selman, Said Al-Hallaj, "2002", [11], studied on a MEH unit analytically. They were derived the governing equations that represent the performance of humidifier, dehumidifier and the collector, mathematically. The study was about three different units, in three different locations (Iraq, Malaysia, Jordan). A simulation was done for evaluating the effects of components of MEH

unit in Malaysia, but with varying sizes of components. A schematic of the desalination unit is indicated in Figure 2.9.

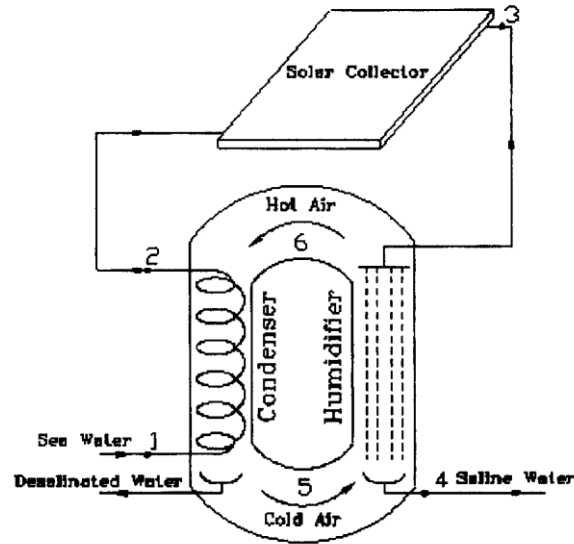


Figure 2-9: Sketch of a Natural Draft Air Circulation MEH Desalination System [11].

The unit built in Malaysia consists of a cylinder with 3 meter long and 0.17 m diameter, as the condenser. The humidifier was made of 6 modules with 0.5 m height. In cross arrangement, wooden thin sheets were combined to form the modules. An electrical heater was used in steady state mode and a solar collector for unsteady state mode. Maximum productivity was obtained for 0.013 kg/s of water flow rate, for a unit consists of a 9m² condenser area, a 3m² collector area, and an 11.9m² humidifier areas.

S. Farsad, A. Behzadmehr, , in “2011”, [12], studied on a HDH desalination unit including two solar collectors, one for air and the other for water heating, a humidifier and a condenser. Figure 2.10 is illustrating the described unit.

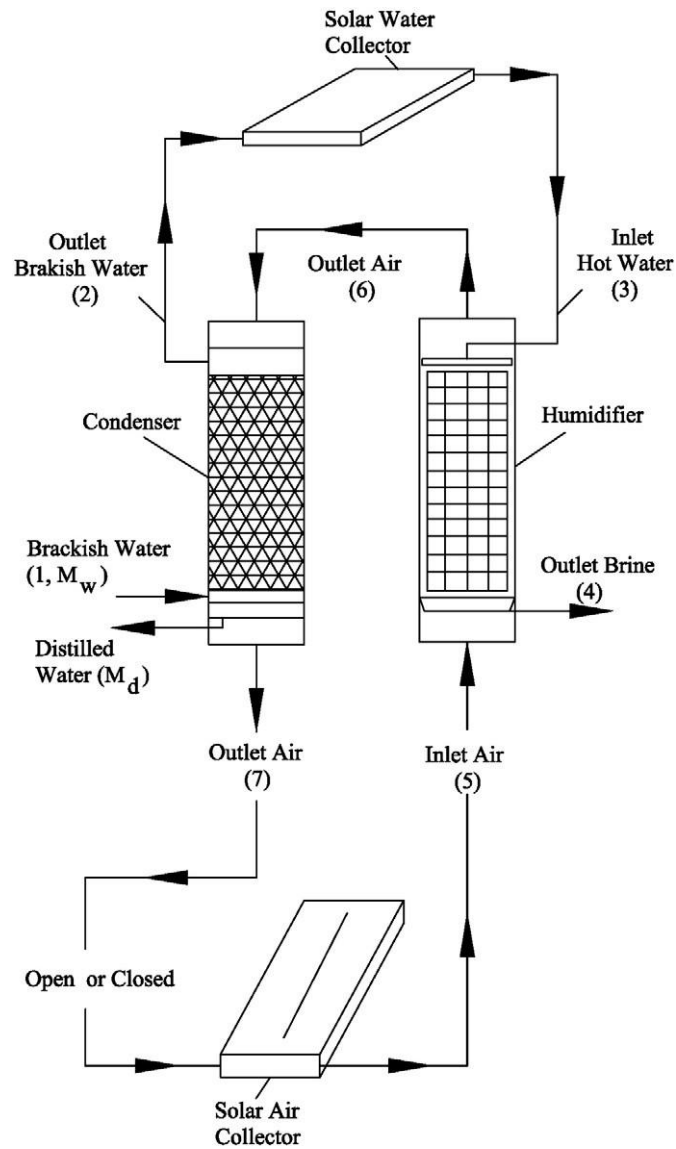


Figure 2-10: Schematic of a Desalination Unit with Air and Water Heating and Closed Water Cycle [12].

Design of experiment method (DOE) was used to discover Sensitivity of the cycle parameters. Mass and energy balance equations were solved numerically to analyze cycle parameters, and the amount of potable water production. It was found that the mass flow rate of water and its temperature, inlet air characteristics, the condenser characteristic parameter, and the total heat flux are the most effective parameters on the cycle performance. The DOE analysis was adopted to show the dependency of these parameters on the fresh water production.

In “2007”, S.M. Soufari, M. Zamen, M. Amidpour, [13], optimized the performance of a HDH desalination unit using mathematical programming. The case under the study was HDH desalination process with a closed, air cycle, using water heating technique. An illustration of the mentioned system is shown in Figure 2.11.

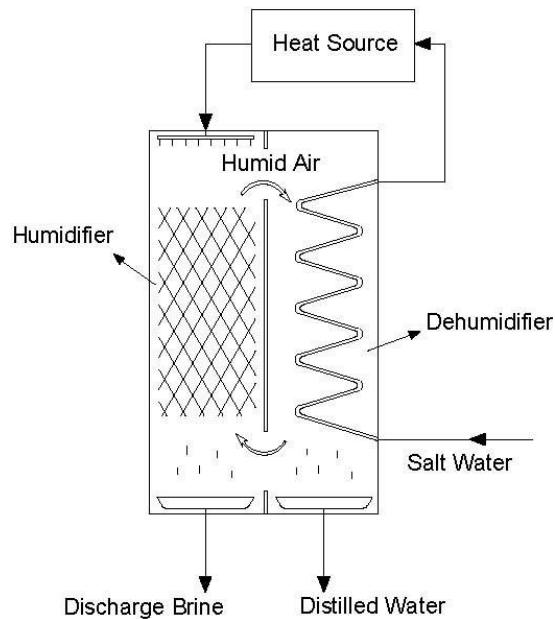


Figure 2-11: Sketch of a Water Heating Closed Air Cycle Desalination Unit [13].

Water to air flow rate ratio (L/G) and the humidifier water inlet temperature was observed to be the most effective parameters on the cycle’s performance. The higher humidifier inlet water temperature and higher L/G ratio was decreasing the required heat transfer area for both humidifier and dehumidifier. It was also observed that, in high humidifier inlet water temperature, water productivity can be increased by recycling humidifier discharge water to the dehumidifier. Recycling will results in smaller humidifier area and larger dehumidifier surface.

Said Al-Hallaj, Sandeep Parekh, M.M. Farid, J.R Selman, [14], in “2005” evaluated the solar HDH desalination unit from the economical point of view. A comprehensive study of the mechanism of HDH process was presented in their report. Comparison of the process costs with all the other solar based desalination techniques was presented by the authors. In this literature, methods of reducing the cost of water production were analyzed. These methods are including; development of more efficient solar collectors, and combining of thermal storage facilities with the solar desalination unit. Reduction of potable water production, up to 20%, is achievable by means of a better evaporation surface, and thinner flat plate heat exchangers on the dehumidifier.

A summary of the cost for the potable water from different solar powered HDH desalination processes are tabulated in Table 2.1.

Table 2-1: Summary of the Cost of Different Solar Base HDH Units [14].

Plant type	Capacity/productivity (m ³ d ⁻¹)	Cost of product water (\$m ⁻³)	Description/reference
Solar-MED	20,000	0.89	Solar pond-MED [16]
	200,000	0.71	
	100,000	0.67–1.44	Solar-pond LT-MED, SEGS-LT MED, troughs-TVC, SEGS-SWRO [17]
	0.151	2.05	Solar boiler-MED [18]
	40	2.15–4.70	Solar hot water storage-MED [19]
	1000	1.20	Solar only with storage [20]
	1000	1.10	Solar-fuel-hybrid [20]
	10,000	0.92	
	100,000	0.69	
	Solar-MEE (FPC)	100	4.00
Solar-MEE (ETC)	100	5.10	
Solar-MED	100	8.3–9.3	Solar thermal-diesel systems [23]
	500	5–6.70	
	1000	3.40–4.40	
Solar-MSF	1	2.84	Complete solar based [24]
	1	1.79	Partial solar [24]
Solar-RO	—	12.05	Solar-PV system [24]
	—	5.70	Solar pond-RO [24]
	—	2.99	Solar-PV [24]
	—	1.80–2.23	Solar thermal [14]
	—	2.75–3.15	Solar-PV [14]

In “2004” Ghazi Al-Enezi, Hisham Ettouney, Nagla Fawzy, [2], carried out an evaluation of the characteristics of a HDH desalination process, as a function of the operation condition. A small capacity prototype was used to evaluate the effects of flow rates of water and air, and the temperature of water stream and cooling water stream temperature. A schematic of the experimental system is indicated in Figure 2.12.

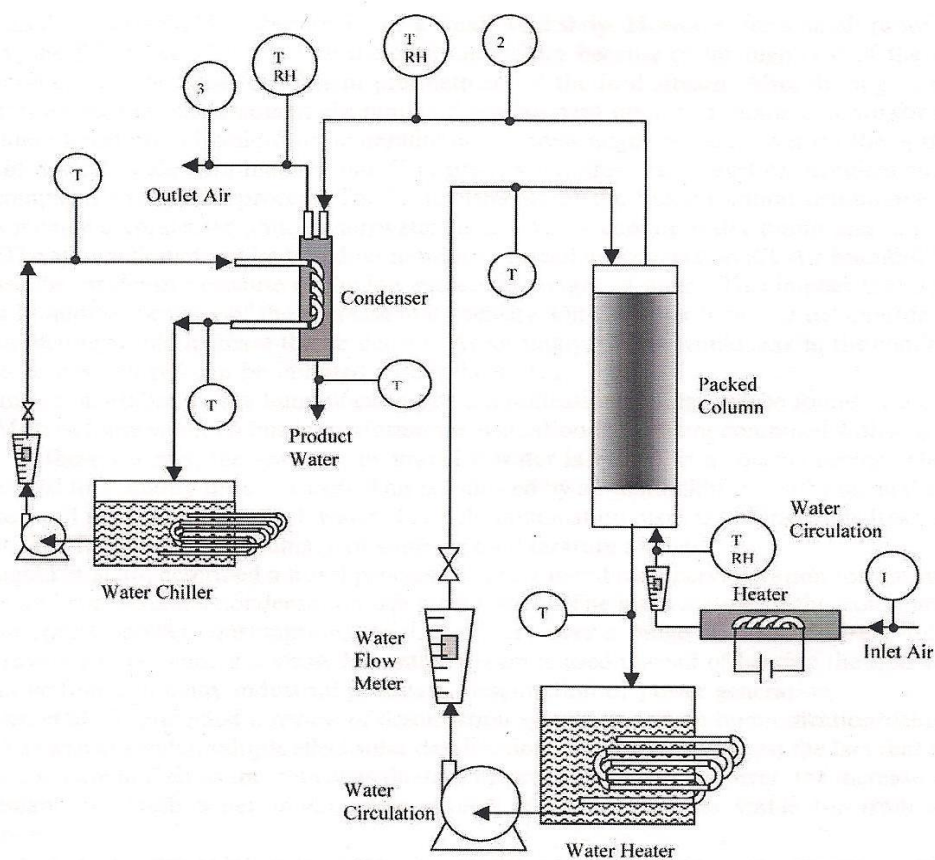


Figure 2-12: A Schematic of Experimental Unit [2].

It was observed that; the highest potable water production is at high, hot water temperature, low cooling water temperature, high air flow rate and low, hot water flow rate. There was a similar pattern to water production rate and the overall heat and mass transfer coefficients.

The present study is mostly based on a study of solar desalination system with cascading evaporation in Northern Cyprus, carried out by R. Kraft, U. Atikol, in “2010”, [4], which it was aimed to supply potable water for a one family household, with simply maintenance and low investment cost. The HDH desalination used in this experiment was consist of a solar air collector with 2 square meter absorption area, a cascading evaporator with total volume of 0.23 cubic meters, and a finned condenser with total volume of 0.1 cubic meters. A schematic of the system is indicated in figure 2.13.

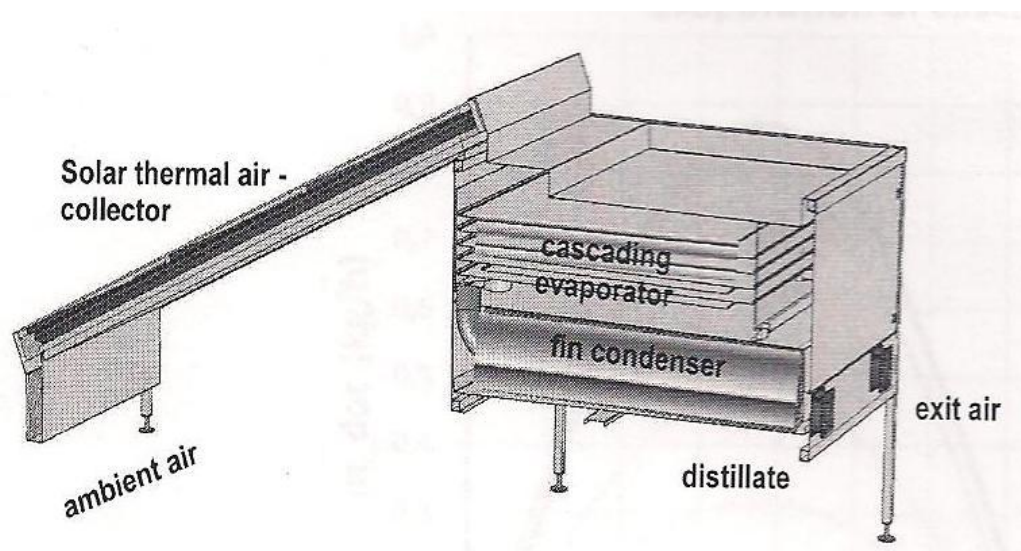


Figure 2-13: A Solar Base HDH Desalination System [4].

The experiment was conducted in Austria and North Cyprus, but the production was not sufficient. Therefore the current experiment is planned to find a solution for the mentioned system.

Chapter 3

REVISION OF THE GOVERNING EQUATIONS

3.1 Introduction

In preceding chapter, it was mentioned that a typical solar humidification dehumidification includes one or two solar heaters, an evaporator and a condenser [9]. Discussing the governing equation for each of them is the object of this chapter. In the unit under study we have a solar air collector, a cascading evaporator and a double pipe, shell and tube, heat exchanger as the condenser. Besides, an electric instant water heater is used to heat up the water. A schematic of the unit is illustrated in Figure 3.1.

In order to simplify the calculation, first of all we split the whole unit, into its three main parts:

1. Solar air collector
2. Cascading evaporator (humidifier)
3. Condenser (dehumidifier)

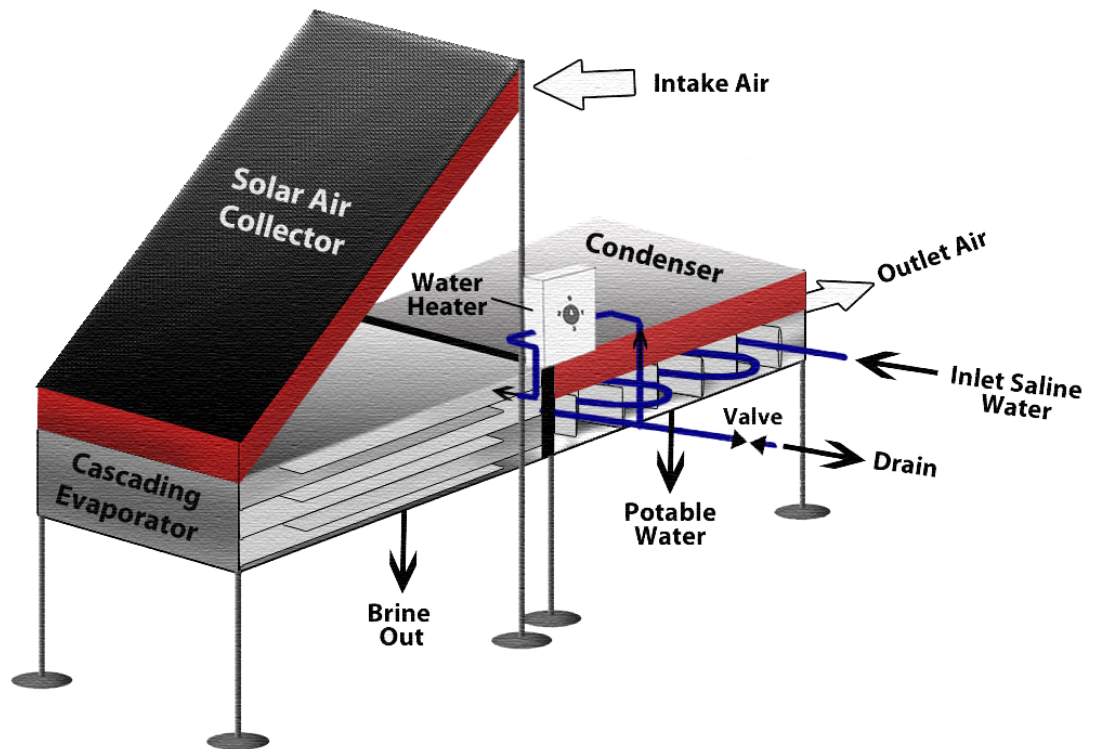


Figure 3-1: Desalination Unit

3.2 Solar Air Collector

Solar air collector is a particular type of heat exchanger that converts the radiation energy to the useful internal energy of transport air [15]. There are two kinds of solar air collectors; flat plate and concentrating collectors. In this study, a flat plate solar air collector is used, which is discussed in following. Figure 3.2 indicates a typical flat plate solar air collector.

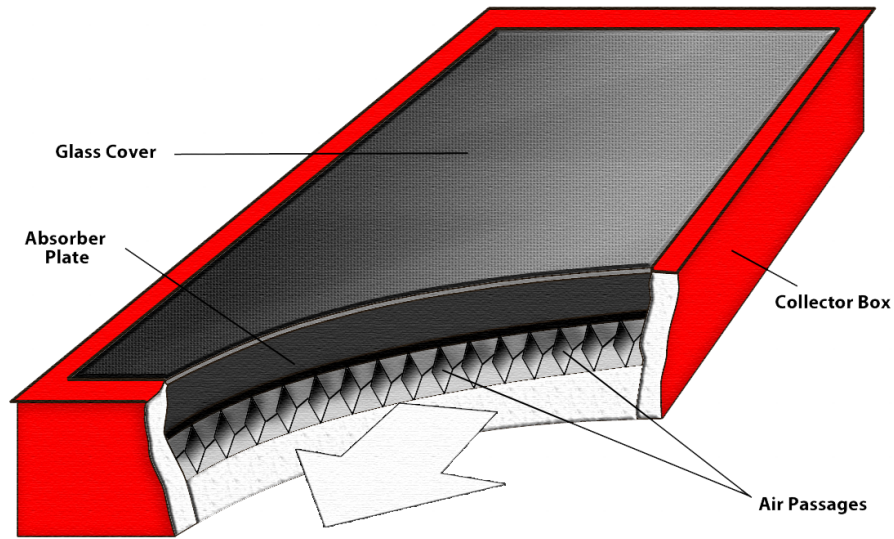


Figure 3-2: Solar Air Collector

3.2.1 Energy Balance

In order to find the outlet temperature of the air from the solar air collector energy balance must be applied on the collector.

Applying an energy balance on each part of collector, and combining the results will give us an equation, which is temperature distribution equation for air in the duct [15].

$$T = \left(\frac{H_a}{U_c} + T_a \right) - \frac{1}{U_c} [H_a - U_c(T_{A,in} - T_a)] \exp \left[-\frac{U_c F' x}{m c_p} \right] \quad (3.1)$$

Where

H_a = Absorbed radiation, [W/m²]

U_c = Collector overall heat loss coefficient, [W/m².K]

$T_{A,in}$ = Inlet air temperature, [K]

T_a = Ambient temperature, [K]

\dot{m} = Mass flow rate of air through the collector, [kg/sec]

c_p = Specific heat of air, [J/kg.K]

$$F' = \text{collector efficiency factor} = \frac{1/U_c}{(1/U_c)+(1/h)} = \frac{h}{h+U_c} \quad (3.2)$$

The outlet temperature of air can be calculated by letting $x = l$ and noting that

$A_c = wl$. Thus

$$T_{A,out} = T_{A,in} + \frac{1}{U_c} [H_a - U_c(T_{A,in} - T_a)] [1 - \exp\left(-\frac{A_c U_c F'}{\dot{m} c_p}\right)] \quad (3.3)$$

This is a general equation for all the collectors with the same configuration. In order to specify this equation for a particular collector, the overall heat loss coefficient of that collector must be substituted in the equation 3.3.

The useful energy gain by the air stream is then

$$Q_u = \dot{m} c_p (T_{A,out} - T_{A,in}) \quad (3.4)$$

Where

$T_{A,out}$ = Outlet air temperature, [C]

Q_u = Total rate of useful energy gain, [W]

It is highly desirable to express the total useful energy gain of the collector in terms of the inlet air temperature, which is known and equal to the ambient temperature. Therefore, it is necessary to define a factor, so called; collector heat removal factor (F_R). Collector heat removal factor is expressed in equation 3.5.

$$F_R = \frac{\dot{m}c_p(T_{A,out}-T_{A,in})}{A_c[H_a-U_c(T_{A,in}-T_a)]} \quad (3.5)$$

Where

A_c = Collector area

Substituting equation 3.4 in equation 3.5 results:

$$Q_u = F_R A_c [H_a - U_c (T_{A,in} - T_a)] \quad (3.6)$$

Where:

A_c = Collector area, [m²]

H_a = Absorbed radiation, [W/m²]

U_c = Collector overall heat loss coefficient, [W/m².K]

$T_{A,in}$ = Inlet air temperature, [K]

T_a = Ambient temperature, [K]

\dot{m} = Mass flow rate of air through the collector, [kg/sec]

The instantaneous efficiency of the collector at any short time interval is simply the ratio of the useful energy gain to the incident radiation at the specific time interval.

$$\eta_c = \frac{Q_u}{A_c H_t} \quad (3.7)$$

Where H_t is the total insolation

3.2.2 Absorbed Solar Radiation

When solar radiation reaches to the collector surface, a major portion of it will transmit through transparent cover and falls on the absorber plate. The absorbed amount of solar radiation depends on the absorptivity of the absorber plate and the transmissivity of the glazing system.

Incident radiation consists of three components; beam radiation, diffuse radiation and ground reflected radiation, and they are incident on the collector surface with different angles. Therefore, they must be taking into account separately.

The total incident radiation on a tilted collector surface is:

$$H_t = H_B R_B + H_d \left(\frac{1+\cos s}{2} \right) + H \rho_g \left(\frac{1-\cos s}{2} \right) \quad (3.8)$$

H_B = Beam radiation on a horizontal surface, [W/m²]

R_B = The beam radiation tilted factor

H_d = Diffuse sky radiation on a horizontal surface, [W/m²]

H = Total radiation on a horizontal surface = $H_B + H_d$

s = Tilted angle

ρ_g = Ground diffuse reflectivity, [W/m²]

Therefore, treating for the three radiation components separately, the absorbed radiation by the collector can be expressed as:

$$H_t = H_B R_B (\tau\alpha)_B + H_d (\tau\alpha)_d \left(\frac{1+\cos s}{2} \right) + H \rho_g (\tau\alpha)_g \left(\frac{1-\cos s}{2} \right) \quad (3.9)$$

Where

$(\tau\alpha)_B$, $(\tau\alpha)_d$ and $(\tau\alpha)_g$ are the transmissivity-absorptivity products for beam, diffuse sky and diffuse ground reflection radiation, respectively.

Ground diffuse reflectivity depends on the ground surface covered by snow, and it is varying from 0.2 for no snow on the ground, to 0.7 for fully snowed ground [15].

3.2.3 Humidity Calculation

Using the solar air collector in a humidification dehumidification system yields another important parameter, which is relative humidity. Relative humidity is the ratio of the total amount of moisture the air holds (m_v) to the amount of moisture that air can hold (m_g) at the same temperature, [16], and it is defined as:

$$\phi = \frac{m_v}{m_g} = \frac{P_v V / R_v T}{P_g V / R_v T} = \frac{P_v}{P_g} \quad (3.10)$$

Where

m_v = Total mass of moisture the air holds, [kg]

m_g = The mass of moisture that air can hold, [kg]

P_v = Partial pressure of water vapor, [kPa]

P_g = Saturation pressure of water, [kPa]

V = Volume, [m³]

R_v = Universal gases constant = 0.287 Kpa.m³ /Kg.K

T = Temperature, [K]

Specific or absolute humidity can be defined as the ratio of mass of water vapor present in a unit mass of dry air, [16]:

$$\omega = \frac{m_v}{m_a} = \frac{P_v V / R_v T}{P_a V / R_a T} = \frac{P_v / R_v}{P_a / R_a} = \frac{0.622 P_v}{P - P_v} \quad (3.11)$$

m_a = Mass of dry air, [kg]

The parameters P_v and P_a , represent the partial pressure of water vapor and that of the air, respectively, and P is the sum of these two partial pressures which present the total pressure.

The partial pressure of water is determined from equation 3.12:

$$P_v = \phi P_g = \phi P_{sat@T} \quad (3.12)$$

Where $P_{sat@T}$ stands on the saturated pressure at a specific temperature of T. Consequently, the partial pressure of air, as previously mentioned, is the difference between the total pressure and the water partial pressure.

As air is travelling through the collector, the temperature of air will rise, but the amount of water vapor remains constant. Therefore, the relative humidity of the air decreases.

Properties of air are known at the collector inlet; consequently, amount of water vapor is measurable from equation 3.10 and the outlet temperature can be computed

from equation 3.3. Therefore, relative humidity and the amount of vapor carrying by air, at the collector outlet are computable.

3.3 Evaporator

The humidifier used in this experiment is a cascading evaporator, which is fed by the heated water from the auxiliary water heater. This device is a kind of instantaneous mass and heat exchanger. Hot air enters to the evaporator and contacts with water in a parallel pattern. The main parameter for the aim of humidification is the amount of water diffused into the air. Known factors are inlet air temperature and humidity, air flow rate and the area of the evaporator, water flow rate is also known. Outlet air temperature and humidity must be compute. The inlet water temperature on the evaporator is equal to the outlet water temperature of condenser.

A schematic of the evaporator with the inlet and outlet flows is illustrated in Figure 3.3.

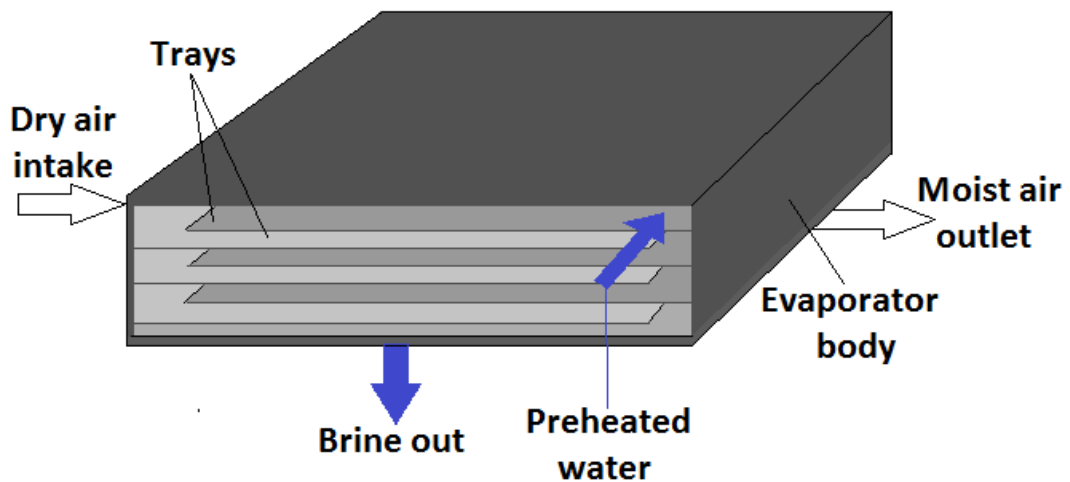


Figure 3-3: Cascading Evaporator

The following assumptions are required to determine the unknown parameters:

1. This is a steady-flow procedure and thus the mass flow rate of dry air remains unvarying during the intact process.
2. Dehydrated air and water vapor are ideal gases.
3. The kinetic and potential energy changes are negligible.

As mentioned previously, air has its own humidity. It means that some water vapor is carrying by air, and because the humidity is known at entrance of evaporator, therefore the mass flow rate of water vapor is computable, where it is a portion of total mass flow rate of air.

Applying the mass and energy balance on the humidifier will result [17]:

$$\dot{m}_{a,in} + \dot{m}_{w,in} = \dot{m}_{a,out} + \dot{m}_{w,out} \quad (3.27)$$

$$\dot{m}_{a,in}h_{a,in} + \dot{m}_{w,in}h_{w,in} + \dot{m}_{v,in}h_{v,in} = \dot{m}_{a,out}h_{a,out} + \dot{m}_{w,out}h_{w,out} + \dot{m}_{v,out}h_{v,out} \quad (3.28)$$

Where

$\dot{m}_{a,in}$ and $\dot{m}_{a,out}$ are mass flow rates of air at the evaporator inlet and outlet, respectively.

$\dot{m}_{w,in}$ and $\dot{m}_{w,out}$ are mass flow rates of water at the evaporator inlet and outlet, respectively.

$\dot{m}_{v,in}$ and $\dot{m}_{v,out}$ are flow rates of water vapor at the evaporator inlet and outlet, respectively.

$h_{a,in}$ and $h_{a,out}$ are presenting enthalpy of the air at inlet and outlet of evaporator, respectively.

$h_{w,in}$ and $h_{w,out}$ are the enthalpies of water at inlet and outlet of evaporator, respectively.

$h_{v,in}$ and $h_{v,out}$ are the water vapor's enthalpies at the inlet and outlet of evaporator, respectively.

Mass diffusion coefficient is a parameter which defines the amount of water diffused into the air in the unit of area at the unit of time [17]. This factor is shown as D, and can be calculated from the equation 3.29:

$$\frac{\dot{m}_a}{\dot{m}_w} (h_{a,in} - h_{a,out}) = \left(\frac{DAV}{\dot{m}_w}\right) \frac{(h_{w,in} - h_{a,out}) - (h_{w,out} - h_{a,in})}{\ln \frac{(h_{w,in} - h_{a,out})}{(h_{w,out} - h_{a,in})}} \quad (3.29)$$

Where

V= The volume of the entire evaporator, [m³]

A= Specific area of evaporation, which is the ratio of evaporation area to the volume of Evaporator, [m]

\dot{m}_a = Mass flow rate of air, [kg/sec]

\dot{m}_w = Mass flow rate of water, [kg/sec]

In the above equation h_a represent the enthalpy of air at the entrance temperature which can be calculated by the equation 3.30. Note that temperatures are in centigrade.

$$h_{dry\ air} = c_p T \quad (3.30)$$

The enthalpy of water vapor is computable using equation 3.31:

$$h_v = 2500.9 + 1.82T \quad (3.31)$$

Therefore the air enthalpy then will be computed with the equation 3.32.

$$h_a = c_p T + \omega h_v \quad (3.32)$$

The water enthalpy is calculated simply from

$$h_{water} = c_p T \quad (3.33)$$

Therefore the rate of mass transfer through the evaporator can be calculated from equation 3.34.

$$\dot{m}_v = -\frac{DA(C_{v2}-C_{v1})}{\Delta x} \quad (3.34)$$

Where, Δx is the thickness of water layer, and the concentration of vapor in air C_v is the ratio of specific humidity over specific volume of air.

$$C_v = \frac{\omega}{v} \quad (3.35)$$

It is also possible to compute the rate of mass transfer in evaporator by applying mass balance:

$$\dot{m}_a \omega_1 + \dot{m}_w = \dot{m}_2 \omega_2 \quad (3.36)$$

$$\Rightarrow \dot{m}_w = \dot{m}_a (\omega_2 - \omega_1) \quad (3.37)$$

While

$$\omega_2 = \frac{0.622 \phi_2 P_{g2}}{P_2 - \phi_2 P_{g2}} \quad (3.38)$$

The amount of heat transfer in the evaporator can be evaluated by calculating the amount of heat transfer rate needed to heat up the water at a constant flow rate.

$$\dot{Q} = \dot{m} c_p \Delta T \quad (3.39)$$

Concept of heat transfer through the evaporator is convection, therefore the rate of heat transfer can be written:

$$\dot{Q} = hA\Delta T \quad (3.40)$$

Where

h = Convection heat transfer coefficient, [W/m².K]

A = The cross sectional area of heat transfer, [m²]

3.4 Condenser

Condenser itself is a double pipe heat exchanger, where the cooling fluid is saline water, and heating fluid is the moist air from the evaporator. Water and air inlet temperatures, besides the outlet temperature of air are known. Outlet water temperature must be compute, which is equal to the inlet water temperature to the evaporator. In order to calculate the outlet, water temperature the equation 4.41, [18], is suggested.

$$q = \dot{m}_c C_c \Delta T_c = \dot{m}_h C_h \Delta T_h \quad (3.41)$$

Where

\dot{m}_c, \dot{m}_h = Mass flow rate of cooling and heating fluid, respectively.

C_c, C_h = Specific heat of coolant and heating fluid, [J/K], respectively.

$\Delta T_c, \Delta T_h$ = Temperature difference of coolant and heating fluid, [C], respectively.

q = The rate heat transfer, [W]

Temperature difference of water in the condenser can be calculated from the above equation. Consequently, the outlet temperature of dehumidifier is computable.

The goal of humidification dehumidification desalination unit is to produce potable water, which it depends strongly on the condenser efficiency. Therefore the condenser is the most vital segment of the whole unit. The thermodynamic of the system is the same as the evaporator. But the cooling and heating fluid are not in contact with each other, thus there would be no mass transfer between them. Figure 3.4 shows the condenser that it is applied for the experiment.

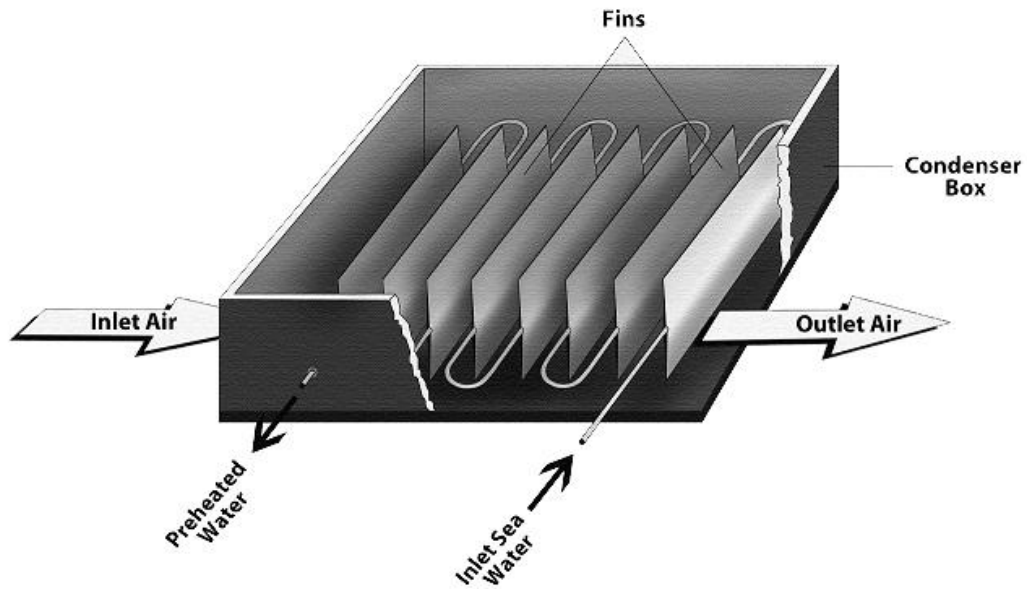


Figure 3-4: Finned Condenser

Before doing any calculation the flow regime inside of the pipes must be defined, it means calculation of Reynolds number is necessary:

$$Re = \frac{\rho u D}{\mu} \quad (3.42)$$

Where

ρ = Density of the fluid, [kg/m³]

u = Velocity of the fluid, [m/s]

D = Diameter of the pipe, [m]

μ = Dynamic viscosity of the fluid, [kg/m.sec]

Heat transfer through the humidifier is mostly conducting with convection heat transfer, but in order to define the heat transfer through the condenser, the overall heat transfer coefficient is required, and that can be calculated with equation 3.43.

$$\frac{1}{UA} = \sum \frac{1}{hA} + \sum R \quad (3.43)$$

Where in this equation parameter R stands on thermal resistance and it is computing by equation 3.44.

U = Overall heat transfer coefficient, [W/m².K]

A = Heat transfer area, [m²]

h = Convection heat transfer coefficient, [W/m².K]

$$R = \frac{x}{k.A} \quad (3.44)$$

x = The wall thickness, [m]

k = The thermal conductivity of the substance, [W/m.K]

A = The overall area of the heat exchanger, [m²]

Accordingly the rate of heat transfer Q can be compute:

$$Q = UA\Delta T_{Lm} \quad (3.45)$$

ΔT_{Lm} , represents the logarithmic mean temperature difference, which is expressed as:

$$\Delta T_{Lm} = \frac{\Delta T_A \Delta T_B}{\ln \left(\frac{\Delta T_A}{\Delta T_B} \right)} \quad (3.46)$$

Where ΔT_A , is the temperature difference among the two streams at end A, and ΔT_B is the temperature difference between the two streams at end B.

There are also some fins assembled on the tubes, in order increase the rate of heat transfer, by increasing the overall heat transfer area. The effect of these fins must be considered in calculations.

There are three different types of fins [18]: first, the fin is too long and the temperature at the end of fin is equal to the ambient temperature. Second, the fin is finite and there is heat transfer at the end of it. Third, the end of fin is insulated, so it is not equal to ambient but there is no heat transfer at the end point. The fin that we are using in this experiment is the third type where insulated at the end point of fin.

Let's say $m^2 = hP/kA$, $\theta = T - T_\infty$, and $\theta_0 = T_0 - T_\infty$. where T_∞ is the ambient temperature, T is the fin temperature and T_0 is the base temperature, the boundary conditions become:

$$\theta = \theta_0 \quad \text{at } x = 0$$

$$\frac{d\theta}{dx} = 0 \quad \text{at } x = L$$

The rate of heat transfer is:

$$q = -kA\theta m \left(\frac{1}{1+e^{-2mL}} - \frac{1}{1+e^{2mL}} \right) = \sqrt{hP/kA}\theta_0 \tanh mL \quad (3.47)$$

Finally the heat transfer ratio for the case of with fin over without fin becomes:

$$\frac{q \text{ with fin}}{q \text{ without fin}} = \frac{\eta_f A_f h \theta_0}{h A_b \theta_0} \quad (3.48)$$

A_f , is the fin area A_b is the base area and the fin efficiency η_f expressed as:

$$\eta_f = \frac{\tanh mL}{mL} \quad (3.49)$$

Thus:

$$\frac{q \text{ with fin}}{q \text{ without fin}} = \frac{\tanh mL}{\sqrt{hP/kA}} \quad (3.50)$$

Measuring the produced amount of potable water is conducted with the dehumidification calculation on the shell side of the condenser. Here we assume that the inlet air temperature is equal to the outlet temperature of water, and the inlet water temperature is equal to the outlet air temperature. Steady state condition is assumed. Therefore, the air flow rate is constant. Kinetic and potential energy changes are negligible. Besides, the air and water are accounted as the ideal gases. The outlet air is also assumed to be saturated, with 100 percent relative humidity.

The enthalpy of saturated liquid water at inlet and outlet state of condenser should be read from water properties table. Also the air properties are available in both states, in psychometric chart.

Therefore, applying mass and energy balance yields:

$$\dot{m}_a = \text{constant} = \frac{\dot{V}}{v} \left[\frac{m^3/min}{m^3/kg \text{ dry air}} \right] \quad (3.51)$$

Where

\dot{V} = Volumetric flow rate, [m³/min]

v = Total mass of moisture in 1 Kg of dry air, [m³/kg]

$$\dot{m}_a \omega_1 = \dot{m}_a \omega_2 + \dot{m}_w \rightarrow \dot{m}_w = \dot{m}_a (\omega_1 - \omega_2) \quad (3.52)$$

Where

\dot{m}_a = Mass flow rate of air, [kg/sec]

\dot{m}_w = Mass flow rate of water, [kg/sec]

ω = Specific humidity

$$\sum_{in} \dot{m} h = \dot{Q}_{out} + \sum_{out} \dot{m} h \rightarrow \dot{Q}_{out} = \dot{m} (h_1 - h_2) - \dot{m}_w h_w \quad (3.53)$$

$$\omega = \frac{0.622 P_v}{P - P_v} \quad (3.54)$$

$$P_v = \phi P_g = \phi P_{sat@T} \quad (3.55)$$

Chapter 4

EXPERIMENTAL SETUP

4.1 System Description

A photograph of the experimental unit is shown in Figure 4.1. The 2 m² solar air heater is located with 20° deviation from true south to the east (surface azimuth angle = -20°), at a tilted angle of 45°. Air enters the solar air heater from the top and leaves from the bottom end into the evaporator.

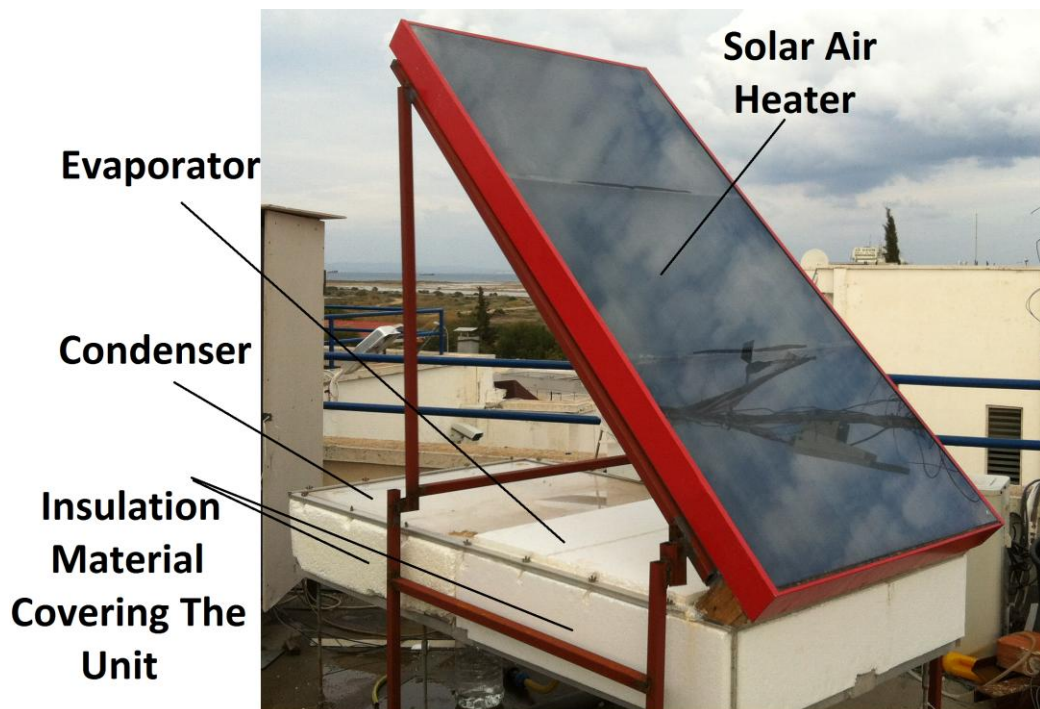


Figure 4-1: HDH Desalination Unit

A cascading evaporator with 0.23 m³ volume and total area of 6 m² is applied to evaporate the water. This area is provided using 6 trays. A shell and tube heat exchanger, with two fined pipes and a shell of 0.12 m³ volume, is chosen to condense

the moist air and produce potable water. Each pipe in the condenser is 18 m long and has 0.635 mm diameter. Just before the condenser, a calibrated water flow meter with a controller valve is installed to adjust the water flow rate. A three way valve is located in between the condenser and evaporator, which is used for adjusting the water flow rate into the evaporator, in order to prevent the flooding phenomena. The extra outlet water of the condenser is drained into the environment.

A 220 volt air blower is fixed on the condenser to suck the air through the air heater into the evaporator and finally over the finned pipes in the condenser. The fan speed and consequently the flow rate of air is adjusted by using a controller switch. The air flow rate is measured by an anemometer (smart sensor AR846) with accuracy of less than 3%. The weather condition is measured using a weather station which measures the air temperature and air humidity. These values are shown on a data acquisition system. Solar irradiance is measured with a pyranometer (eppley radiometer psp) with linearity of $\pm 0.5\%$ from 0 to 2800 W/m^2 . Seven T-type thermocouples are used in order to measure the temperatures of the inlet hot air into the evaporator; inlet moist air into the condenser, outlet water of the evaporator, outlet moist air from the condenser, inlet cooling water into the condenser, outlet water from the condenser and inlet heated water into the evaporator. the temperature reading were recorded by a digital thermometer (HHM2-IR digital multimeter/thermometer) with accuracy of $\pm 1.0^\circ\text{C}$. All the devices and equipments are indicated in Figures 4.2 to 4.9

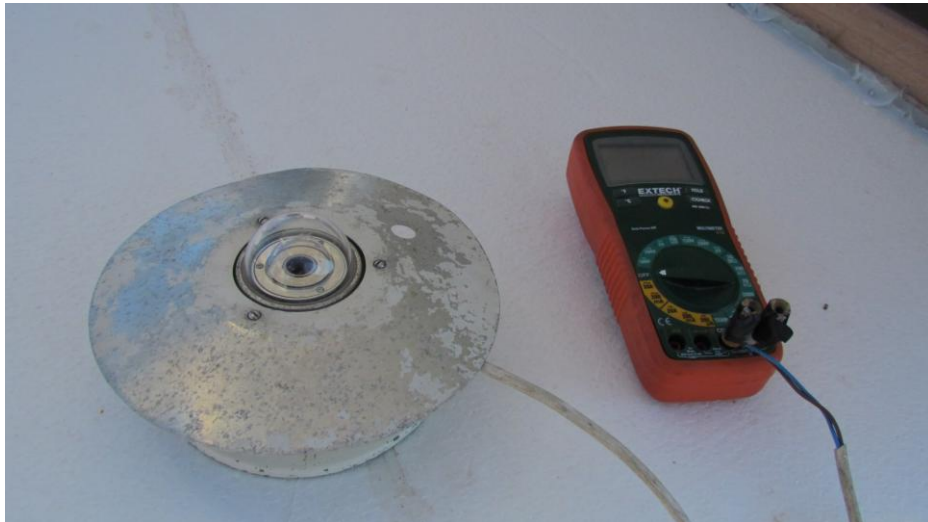


Figure 4-2: Pyranometer



Figure 4-3: Water Flow Meter



Figure 4-4: Air Flow Meter (Anemometer)



Figure 4-5: Digital Thermometer



Figure 4-6: Fan



Figure 4-7: Air Collector

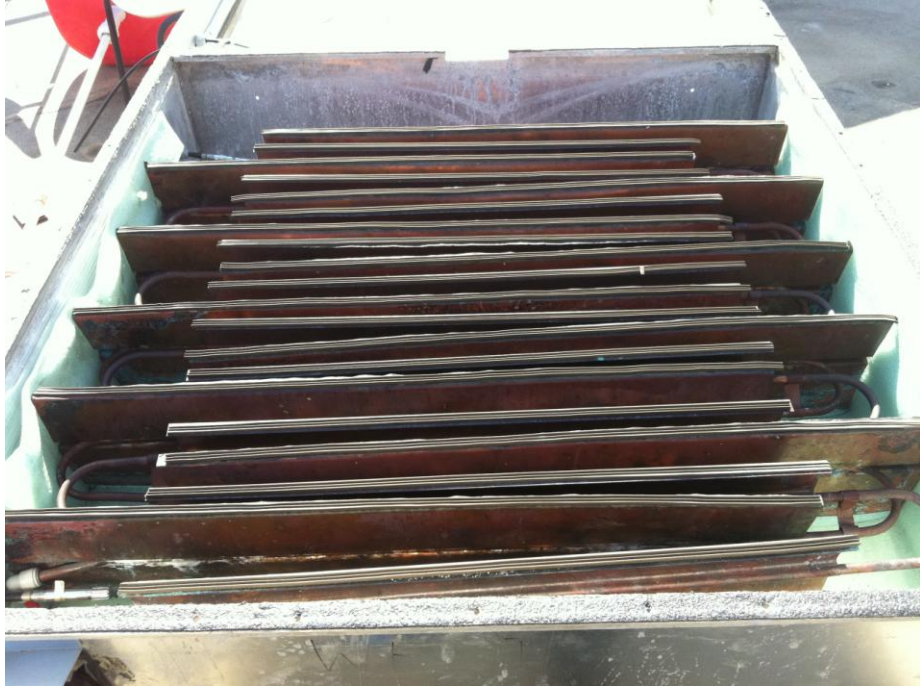


Figure 4-8: Condenser

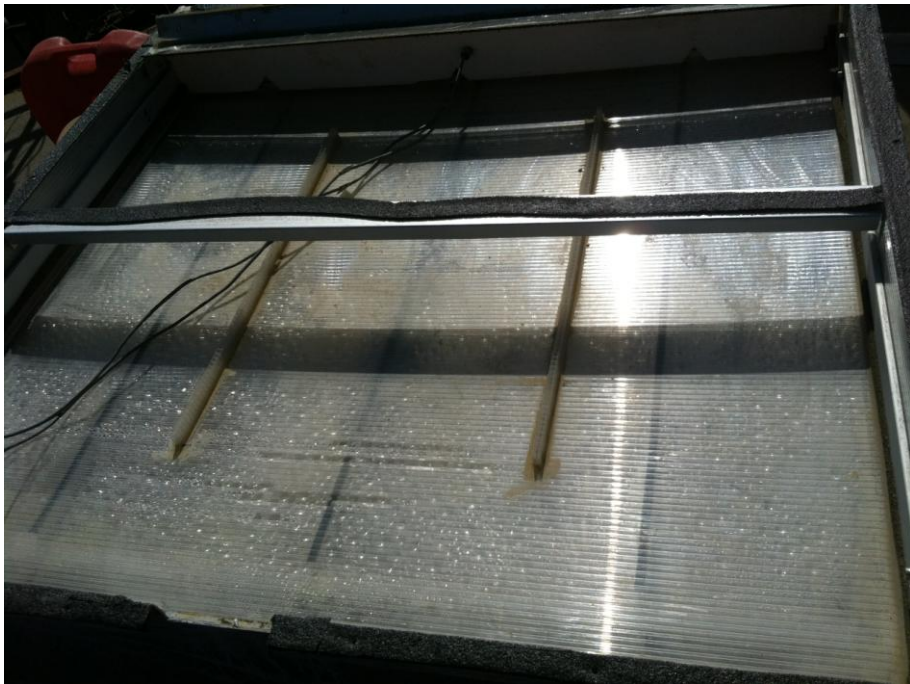


Figure 4-9: Evaporator



Figure 4-10: Water Heater

Water heating technique was not applied at the beginning of the experiment. Therefore the energy of evaporation was not given to the system. Besides, the specific heat of water is approximately 4 times more than that of air. Therefore, in case of mixing the air and water streams, the mixture temperature will be near the water temperature. In HDH desalination system, while only air heating technique is applied, the moist air temperature is only slightly more than the temperature of entering water into the condenser, which leads to zero production of potable water. In order to solve this problem the temperature difference between the heating and cooling fluids into the evaporator must be increased. Increasing the temperature of inlet water into the evaporator is required to increase the temperature difference around the dehumidifier. For this matter an auxiliary electrical water heater (7250 W) is installed on the water pipe, connecting the condenser with the evaporator.

4.2 Uncertainty analysis

In forgoing section the accuracy of devices were mentioned, in this part the theory related to the uncerainity analysis is presented. First for the efficiency of solar air collector we have

$$\eta_c = \frac{\dot{m}c_p\Delta T}{A_c H_t} \quad (4.1)$$

$$\dot{m} = \rho \dot{V} \quad (4.2)$$

\dot{V} is the volumetric flow rate of air which is measured using the previously mentioned anemometer.

Therefor the uncertainty for the mass flow rate is as follow:

$$\frac{\omega_{\dot{m}_a}}{\dot{m}_a} = \left[\left(\frac{\omega_{T_a}}{T_a} \right)^2 + \left(\frac{\omega_{Q_a}}{Q_a} \right)^2 \right]^{1/2} \quad (4.3)$$

Thus

$$\frac{\omega_{\eta_c}}{\eta_c} = \left[\left(\frac{\omega_{\dot{m}_a}}{\dot{m}_a} \right)^2 + \left(\frac{\omega_{\Delta T}}{\Delta T} \right)^2 + \left(\frac{\omega_{H_t}}{H_t} \right)^2 \right]^{1/2} \quad (4.4)$$

Chapter 5

RESULTS AND DISCUSSION

Most of the energy gained by the solar air collector is consumed to heat up the water in the evaporator before saturation. Dramatic decrease in temperature of the moist air causes decrease in the potable water production. The thermal performance of the system without using auxiliary water heater in a typical day of December with the variation of irradiance illustrated in figure 5.1, is shown in table 5.1. it can be seen that the temperature difference between the cooling water into the condenser and the moist air into the condenser is too low leading to failure in water production.

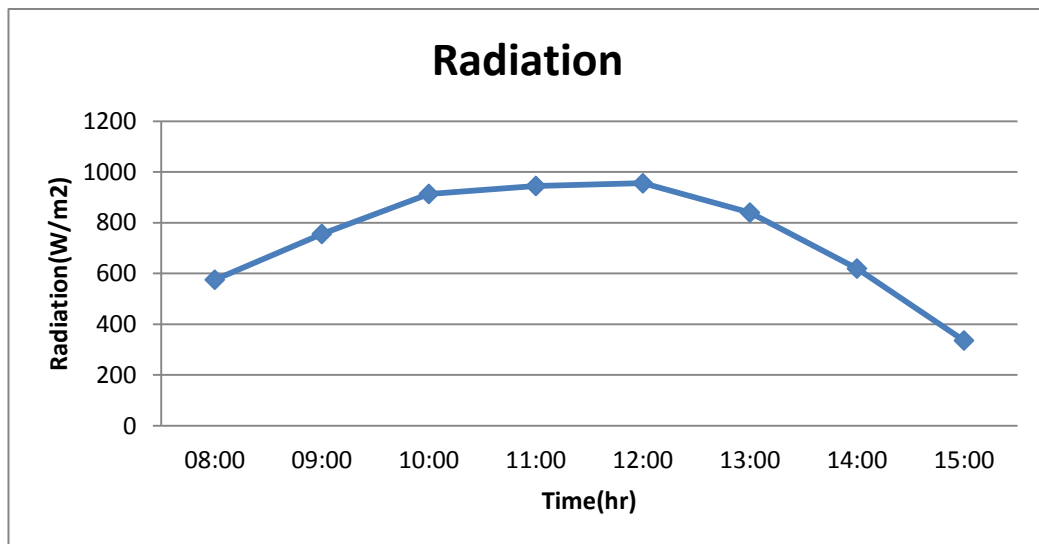


Figure 5-1: Insolation on the Collector Surface during December 21st

Table 5-1: The Temperatures of Air and Water Streams at Operating Conditions on December 21th

t	R W/m ²	T _{amb} °C	H _{amb} %	T _{a,eva,in} °C	T _{a,eva,out} °C	T _{w,eva,out} °C	T _{a,cond,out} °C	T _{w,cond,in} °C	T _{w,cond,out} °C	T _{w,eva,in} °C
8:00	577.5	11	94	27	14	13.5	15.5	13.5	14	14
9:00	756	14	87	40	15.5	15.5	18	15	15.5	15.5
10:00	913.5	18	66	53	18	17.8	19.5	16.3	16.5	16.5
11:00	945	19.5	54	58	20	19.8	19.5	16.5	16.7	16.7
12:00	955.5	19.7	48	60	21	20.5	19.7	16.7	16.9	16.9
13:00	840	19.8	46	54	21.7	21	20.2	16.6	16.8	16.8
14:00	619.5	19.6	46	49	21.5	21.2	19.8	16.4	16.6	16.6
15:00	336	19.4	49	33	21.6	21.2	19.7	16.2	16.4	16.4
ave	742.8	17.6	61.2	46.7	19.2	18.8	19	15.9	16.2	16.2

To solve this problem we need to increase the moist air temperature. In order to increase the moist air temperature the temperature of inlet water into the evaporator must be increased. Therefore, an auxiliary heater is required to heat up the water before it enters to the evaporator. For this goal, an electric water heater with 7250 W, power has used. This water heater is working just when the water flow rate is 4 Lt/min or more, and the flow rate required for the evaporator is 1 Lt/min. Therefore we are running this heater just 15 minutes in an hour.

Applying the above mentioned water heater leads the system to get the results tabulated in Table 5.2.

Table 5-2: The Measured Values for December 27th

t	R W/m ²	T _{amb} °C	H _{amb} %	T _{a,eva,in} °C	T _{a,eva,out} °C	T _{w,eva,out} °C	T _{a,cond,out} °C	T _{w,cond,in} °C	T _{w,cond,out} °C	T _{w,eva,in} °C	Pr Lit
8:00	441	6	94	17	8.5	9.5	8.3	8.2	8.5	48	0.08
9:00	735	9.8	74	33.5	34.2	34.3	11	9.5	12.8	52	0.14
10:00	840	13.2	68	49	39	40	14	11	15.6	53	0.21
11:00	955.5	15	58	51.2	39	40.5	13.5	11	16	55	0.24
12:00	976.5	15	54	62	39	41.5	13.9	10.5	16.1	56	0.26
13:00	819	15.2	50	50	40	42	14	11	16	55	0.26
14:00	630	15.2	50	46	39	42	14.1	10.8	15.9	54	0.23
15:00	346	15.2	52	38	37	38.2	14	10.6	15.8	52	0.22
ave	717.8	13	62.5	43.3	34.5	36	12.8	10.3	14.6	53.1	Tot= 1.66

As it illustrated in table 5-2, the temperature difference of the air in the condenser is 23.2°C, which results in production of 1.66 Lt of potable water During the December 27th. Air flow rate and water flow rate were, 2 m³/min and 6 Lt/min, respectively, and the flow rate of hot water to the evaporator was 1 Lt/min. The inlet water temperature of the evaporator was adjusted on 55°C.

The variation of radiation on December 27th, during the day time is indicated in the Figure 5.2. In Figure 5.3 variation of water production during the day time is shown.

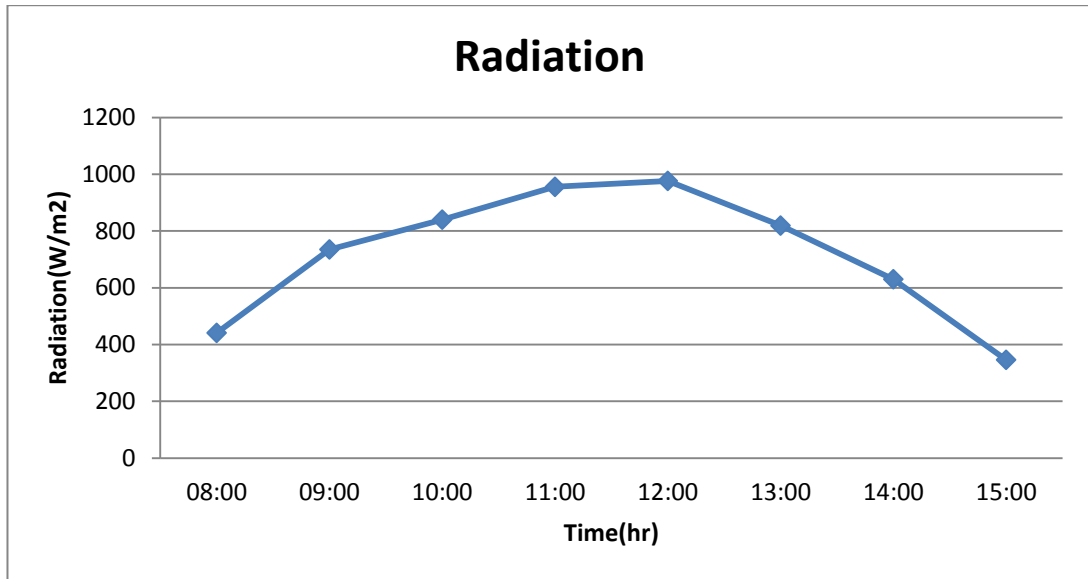


Figure 5-2: Total Radiation on December 27th

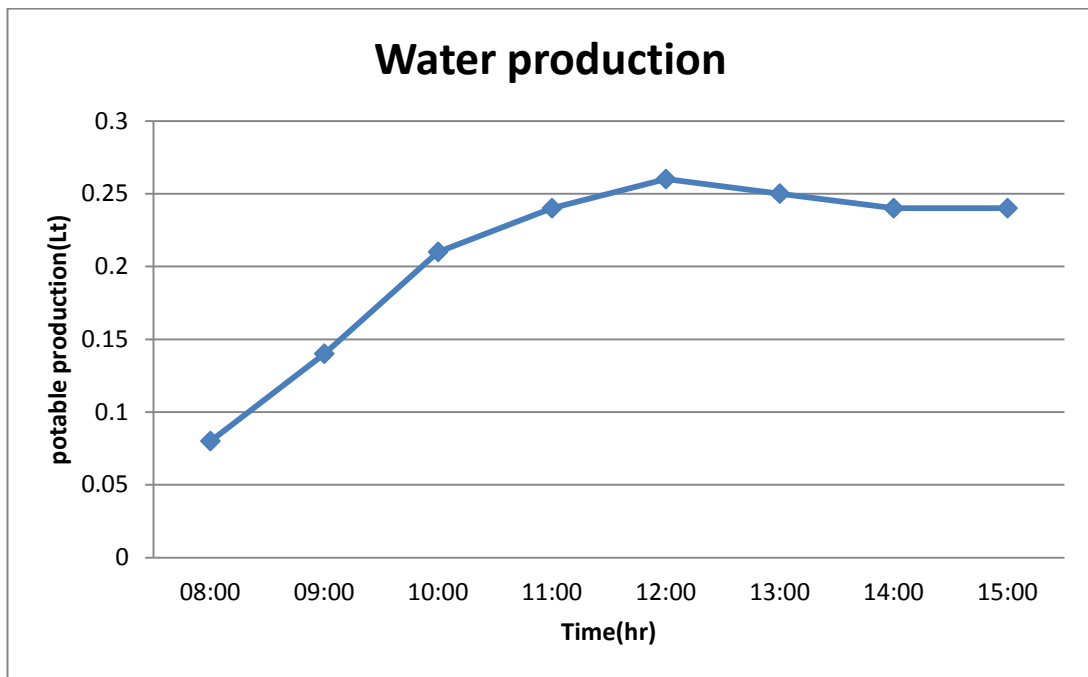


Figure 5-3: Water Production versus Time on December 27th

The humidity of hot and dry inlet air can be computed using the psychrometric chart, theoretically. The average value of the relative humidity from table 5.2 for the inlet dry air to the evaporator is 10%. See appendix (Figure A.1) for the psychrometric chart in SI units.

In Figure 5.4 the hourly water production versus the total rate of energy gained by the unit is indicated.

Rate of energy gained for air and water stream can be calculated from equations 3.4 and 3.39:

$$\dot{Q}_T = (\dot{m}c_p)_W\Delta T_W + (\dot{m}c_p)_A\Delta T_A \quad (5.1)$$

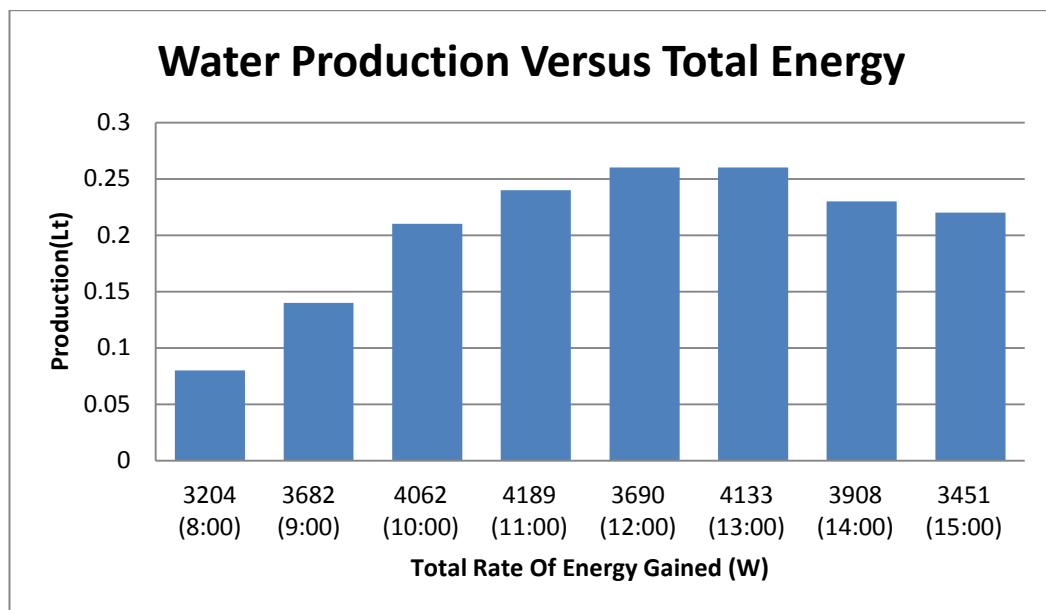


Figure 5-4: Water Production versus Total Rate of Energy Gained On December 27th, (Total Energy = Solar Energy + Electrical Energy)

For December 28th, the flow rate of water into the evaporator was adjusted on 1 Lt/min, and the air flow rate was 2 m³/min. The flow rate of entering water into the condenser decreased to be 4 Lt/min. The evaporator inlet water temperature was adjusted on 55°C. This change results with decreasing the water production to 1.11 Lt for the whole day. The measured values for December 28th are tabulated in Table 5.3.

Table 5-3: The Measured Values for December 28th

t	Rad W/m ²	T _{amb} °C	H _{amb} %	T _{a,eva,in} °C	T _{a,eva,out} °C	T _{w,eva,out} °C	T _{a,cond,out} °C	T _{w,cond,in} °C	T _{w,cond,out} °C	T _{w,eva,in} °C	Pr Lit
8:00	514.5	6.3	87	18.5	6.5	9	8.2	8.5	8	52	0.06
9:00	756	9	77	35	29	30	15	13	14	54	0.12
10:00	955.5	12.9	75	53	41	42.5	16.8	13.2	17	54	0.14
11:00	1008	15	63	60.5	42.3	44	18.2	13.4	17.5	55	0.16
12:00	1029	16.1	51	62.5	42.5	44.1	19.6	14	19	55	0.16
13:00	840	16.7	47	58	41.5	42.8	20.5	13.8	19.8	55.5	0.17
14:00	651	15.9	51	54	41	40.7	20	13.5	19.1	55	0.15
15:00	357	15.5	57	43	40	40.3	20.2	12	19.5	56.5	0.15
ave	763.81	13.42	63.5	48	35.5	36.7	17.31	11.42	16.74	54.6	Tot= 1.11

Comparison of table 5.2 and 5.3 shows that although the average radiation increased on December 28th, but the production is decreased. Decreasing in production from 1.66 Lt on December 27th to 1.11 Lt on December 28th is because of decreasing in water flow rate into the condenser. The air temperature difference in the condenser reduced to 18.2°C. Therefore, while we are decreasing the water flow rate, air flow rate must be decreased proportionally to keep the production in an acceptable level.

The variation of total radiation on the collector surface is presented in Figure 5.5. Besides, in Figure 5.6, hourly changing of the water production is indicated.

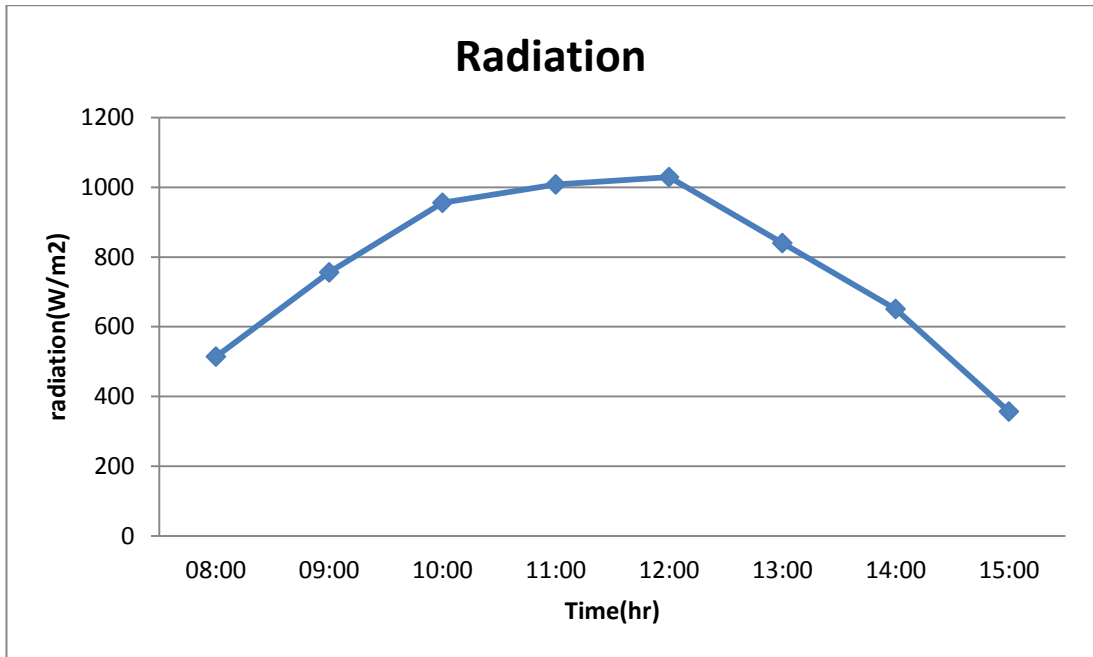


Figure 5-5: Variation of Insolation during the Day of December 28th

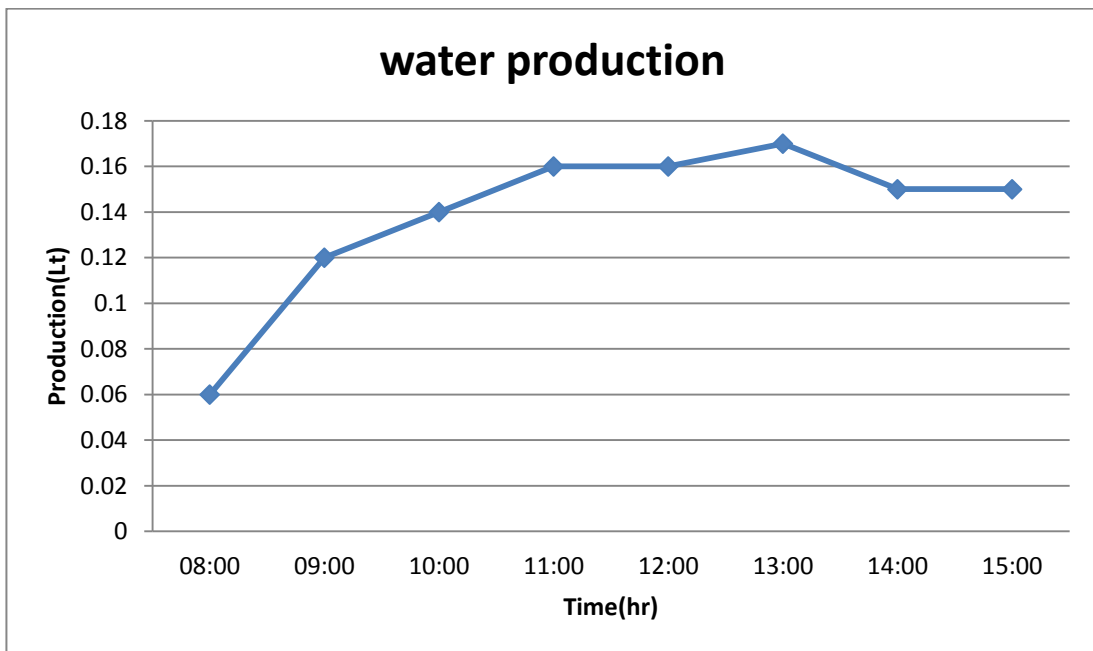


Figure 5-6: Variation of Water Production during the Day of December 28th

According to the Table 5.3, the average temperature of dry air is 48°C. The average values of ambient humidity and ambient temperature are 63.5% and 13.42°C, respectively. Therefore, relative humidity of the dry air from the psychrometric chart is 8.7%.

The variation of water production versus the total rate of energy gained by the whole unit is illustrated in Figure 5.7

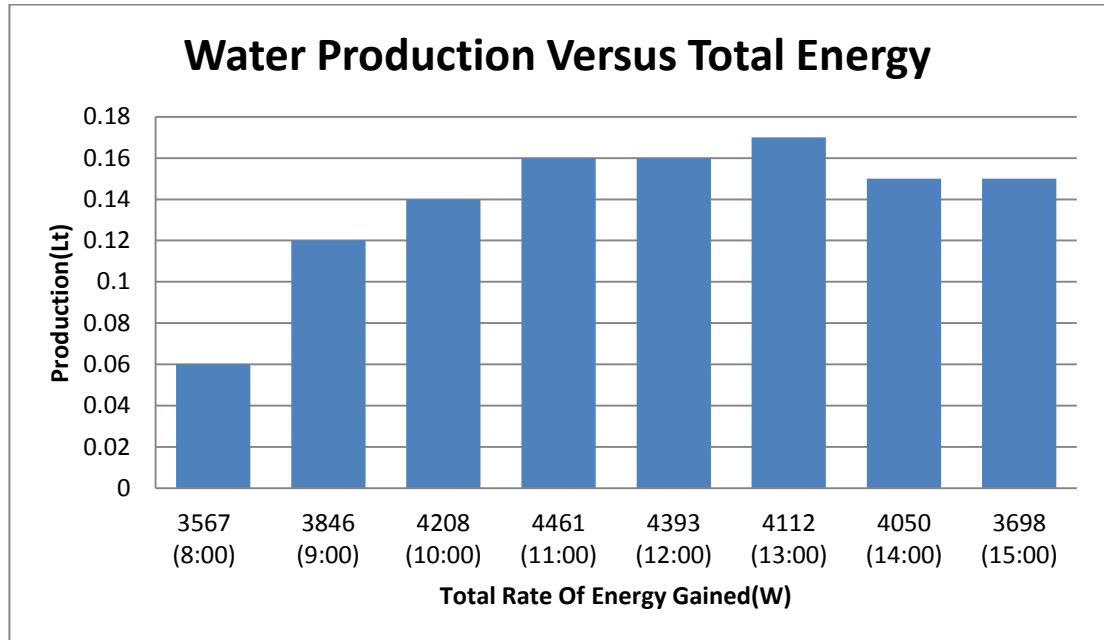


Figure 5-7: Water Production versus Total Rate of Energy Gained On December 28th, (Total Energy = Solar Energy + Electrical Energy)

As it mentioned earlier, while the water flow rate is decreasing, the air flow rate must be decreased as well in order to maintain the water production at a tolerable level. The experiment during December 29th is conducted with the same condition as December 28th, but the air flow rate is dropped to 1.5 m³/min. Adjusting this flow rate for air, conveys the results of Table 5.4.

Table 5-4: Measured Values of December 29th

t	Rad W/m ²	T _{amb} °C	H _{amb} %	T _{a,eva,in} °C	T _{a,eva,out} °C	T _{w,eva,out} °C	T _{a,cond,out} °C	T _{w,cond,in} °C	T _{w,cond,out} °C	T _{w,eva,in} °C	Pr Lit
8:00	504	5.5	91	20	7.8	10.9	7.8	7.4	7.8	54	0.18
9:00	756	8.2	85	34	24	30	10	8	9.6	55	0.29
10:00	903	12.5	70	49.5	39.5	43	14.3	13.4	17.9	56	0.38
11:00	955.5	14.8	59	50	44	47	15.5	13	18.9	56.4	0.42
12:00	976.5	15.5	58	62	46	48	15.1	13.4	19.8	55.5	0.46
13:00	840	15.7	62	58	43	45.5	14.8	13.5	19.9	55.8	0.47
14:00	630	15.5	60.5	55	45	48	14.5	13.3	18.8	57	0.45
15:00	357	15.6	58	42	40.6	43	13.5	13	18.7	56	0.45
ave	740.2	12.9	67.9	46.3	36.2	39.4	13.18	11.87	16.42	55.7	Tot= 3.1

Comparison of the obtained results from table 5.4, with the previous results shows that reducing in air flow rate will result in increasing the moist air temperature difference in the condenser, consequently increases the potable water production.

Variation of total irradiance on the absorber surface of the collector on December 29th is illustrated in Figure 5.8. In Figure 5.9, the hourly production of water during the day of December 29th is drowned. Figure 5.10 shows the amount of potable water produced on December 29th.

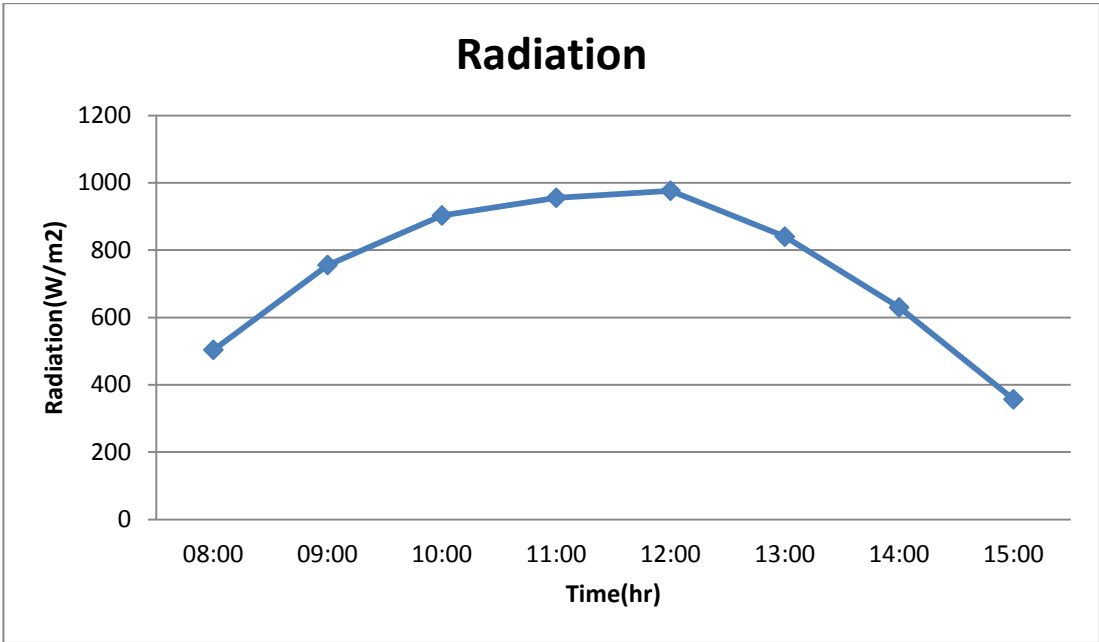


Figure 5-8: Variation of Irradiance during December 29th

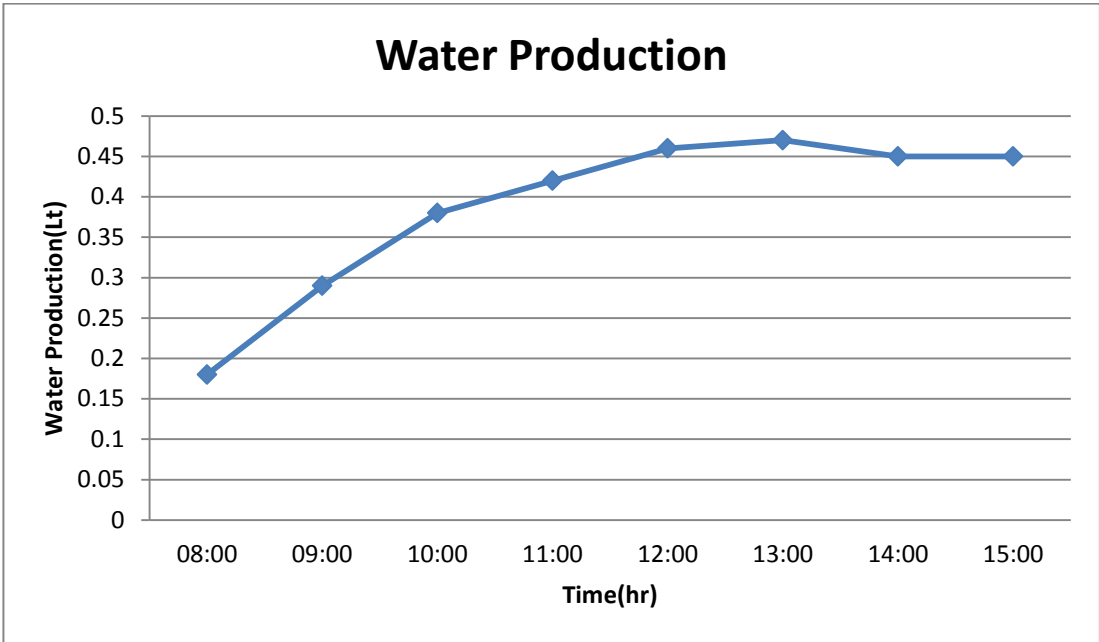


Figure 5-9: Hourly Water Production on December 29th

The value of relative humidity of dry air can be calculated to be 10.1%, using the psychometric chart and the average values of the ambient humidity and temperature.

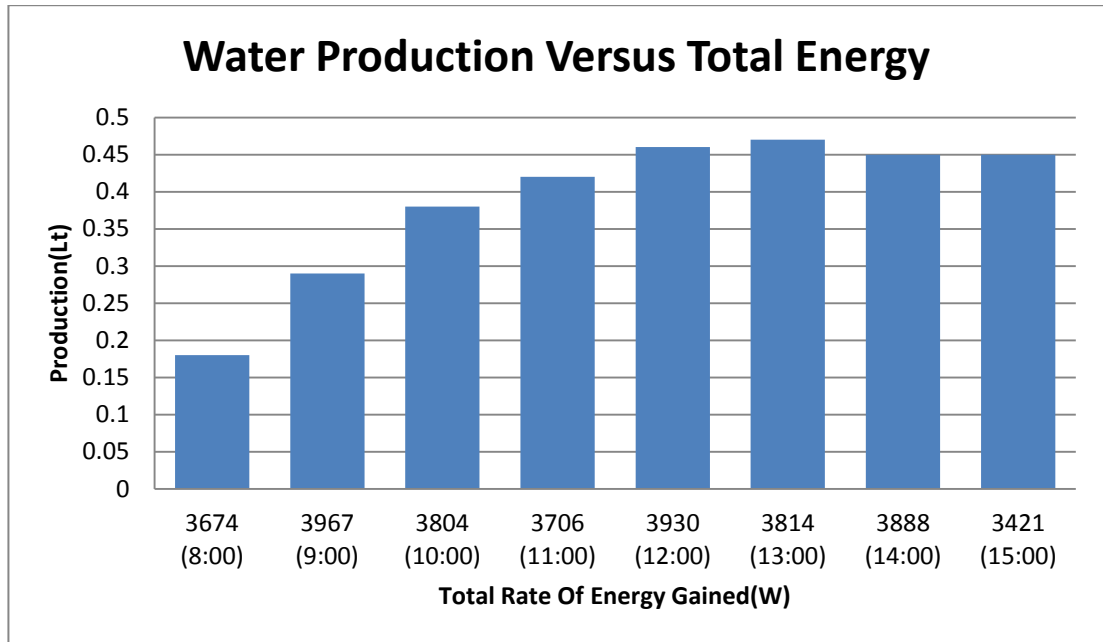


Figure 5-10: Water Production versus Total Rate of Energy Gained On December 29th, (Total Energy = Solar Energy + Electrical Energy)

As it mentioned in this chapter, an auxiliary water heater is used to provide the required temperature of water. Decreasing in water temperature will affect the rate of water production, indeed. For January 4th, the experiment with the water flow rate of 6 Lt/min and air flow rate of 2 m³/min is repeated. Whilst, the water temperature is reduced to approximately 35°C. The results of the experiment are indicated in Table 5.5.

Table 5-5: Measured Values of January 4th

T	Rad W/m ²	T _{amb} °C	H _{amb} %	T _{a,eva,in} °C	T _{a,eva,out} °C	T _{w,eva,out} °C	T _{a,cond,out} °C	T _{w,cond,in} °C	T _{w,cond,out} °C	T _{w,eva,in} °C	Pr Lit
8:00	462	7.8	92	26	12.3	16.9	8.7	7.3	7.7	34	0.03
9:00	756	11.3	83	33	22.7	25.6	15.6	9.2	12.8	37	0.11
10:00	913.5	15.9	69	47	28.9	31.3	16.1	12.5	16.3	37.5	0.13
11:00	934.5	16.1	65	50	30.6	34	15.9	13	16.8	38.3	0.15
12:00	955.5	17	58	52	31.8	34.4	16.1	13.9	17.3	38.4	0.16
13:00	903	17.2	52	42	29	32	16	13.6	15.8	38.1	0.15
14:00	661.5	15.8	63	43	32	33.5	15.4	14	15.3	38.9	0.15
15:00	336	15.6	60	36	31	33	15.9	13.9	15.1	38.2	0.14
Ave	740.2	14.6	67.7	41.1	27.3	30.1	14.9	12.6	14.6	37.6	Tot= 1.02

As the table 5.5 implies by decreasing the water temperature, rate of water production will decrease. The air temperature difference in the condenser is measured to be 12.4, and this is the reason of detraction in water production. Variation of radiation on the collector surface is illustrated in Figure 5.11. The variation of water production during the day of January 4th is illustrated in Figure 5.12. The water production versus total rate of energy gained is indicated in Figure 5.13.

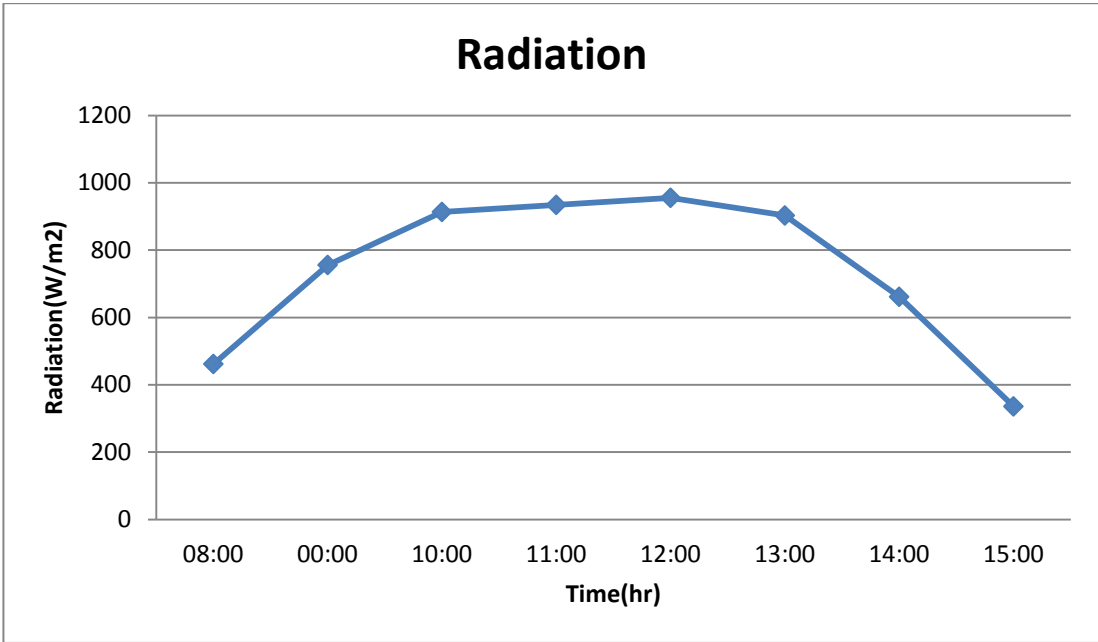


Figure 5-11: Hourly Variation of Irradiance during January 4th

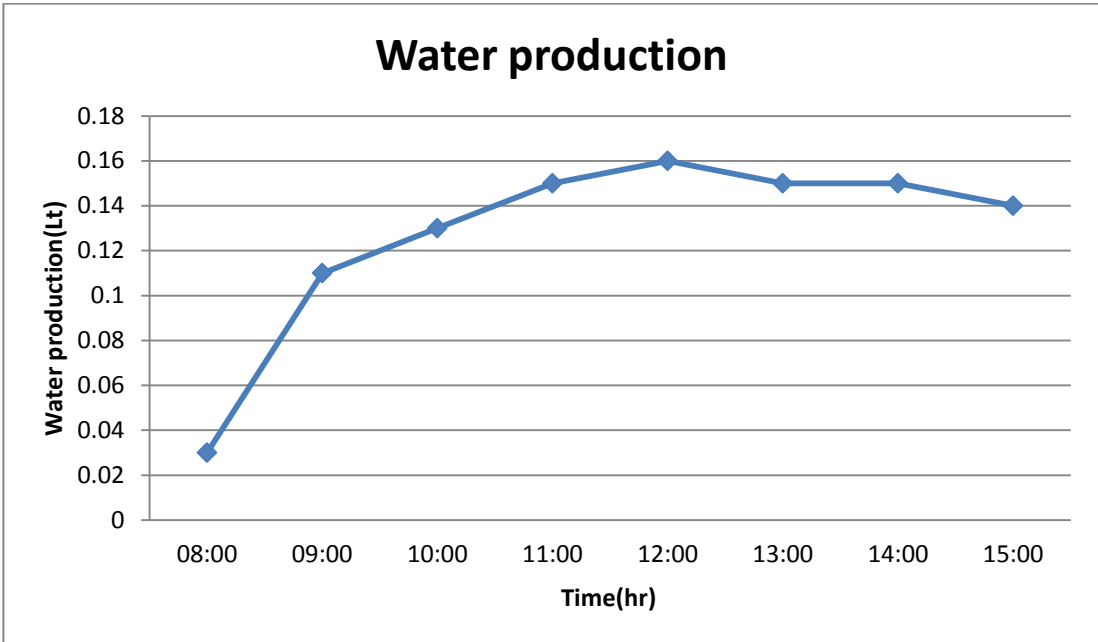


Figure 5-12: Hourly Production of Water during January 4th

Using psychrometric chart in order to calculate the relative humidity of dry air gives the relative humidity of 15.1%.

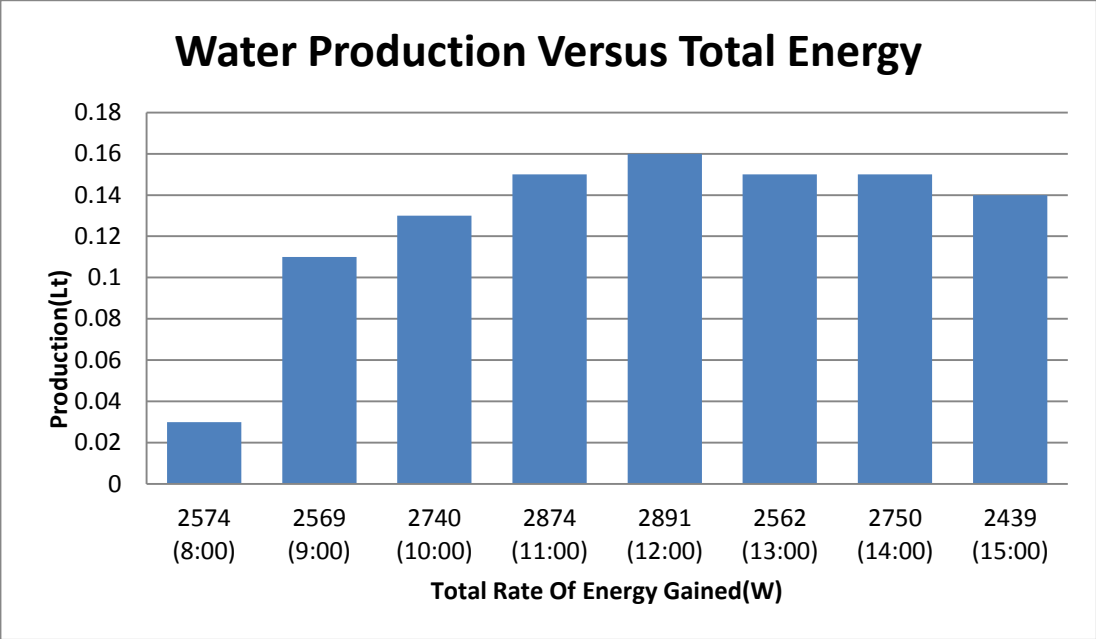


Figure 5-13: Water Production versus Total Rate of Energy Gained On January 4th,
(Total Energy = Solar Energy + Electrical Energy)

On January 5th the experiment is repeated by changing the water flow rate to 4 Lt/min, while the other variables are kept the same as January 4th. The obtained results of the empiric for January 5th are tabulated in Table 5.6.

Table 5-6: Measured Values of January 5th

t	Rad W/m ²	T _{amb} °C	H _{amb} %	T _{a,eva,in} °C	T _{a,eva,out} °C	T _{w,eva,out} °C	T _{a,cond,out} °C	T _{w,cond,in} °C	T _{w,cond,out} °C	T _{w,eva,in} °C	Pr Lit
8:00	441	7	93	24	12	17	9.1	7.6	7.8	34	0.02
9:00	714	11	85	30.7	24.1	27.9	16.5	9.4	13.5	34	0.08
10:00	892.5	15.5	67	45.2	27.2	30.3	16.2	11.8	17.5	35.1	0.1
11:00	934.5	16.4	60	52.8	31.5	34.1	17.9	13.6	17.3	35.8	0.13
12:00	924	16.2	64	45	31.7	33.2	18.1	13.3	17.2	35.4	0.12
13:00	325.5	16	61	33	29	32.3	17.5	12	16.1	35.2	0.11
14:00	42	15.6	66	27.5	27.1	31.9	17.3	11.8	15.6	35.4	0.11
15:00	21	15	65	18.6	26	27.5	16.9	11.7	15.3	35.1	0.1
ave	536.8	14.1	70.1	34.6	26.1	29.3	16.2	11.4	15	35	Tot= 0.77

Noting to the obtained values in table 5.6, shows that although decreasing the water flow rate results with increasing in temperature difference of water in the condenser, but, on the other hand it causes the reduction of air temperature difference in the condenser. Consequently, the water production is reduced to 0.77 Lt/day.

As we are doing the experiment in winter, escaping from clouds is impossible. Impressive drop of irradiance is because of the cloudy weather on January 5th. But as the table 5.6 implies the rate of water production did not reduce significantly. Besides, changing in the outlet moist air temperature from the evaporator was not high. It means that the temperature of outlet air from the evaporator mostly depends on the water temperature.

The variation of irradiance through the day of January 5th is illustrated in Figure 5.14.

Figure 5.15 shows the potable water production during the same day. Figure 5.16,

indicates the water production versus total rate of energy gained by the whole unit.

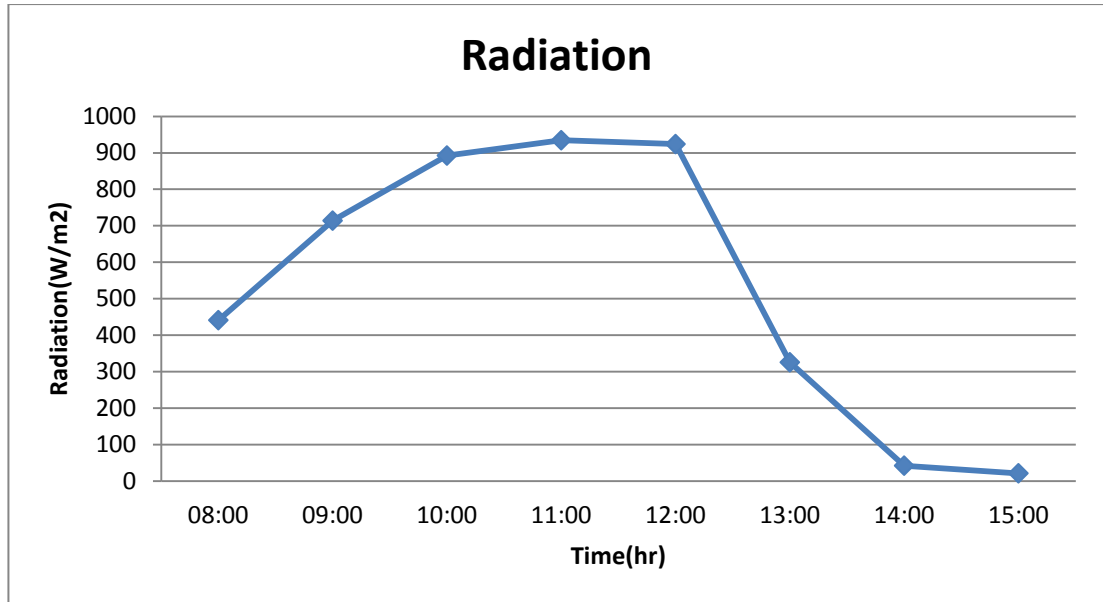


Figure 5-14: Hourly Variation of Insolation on January 5th

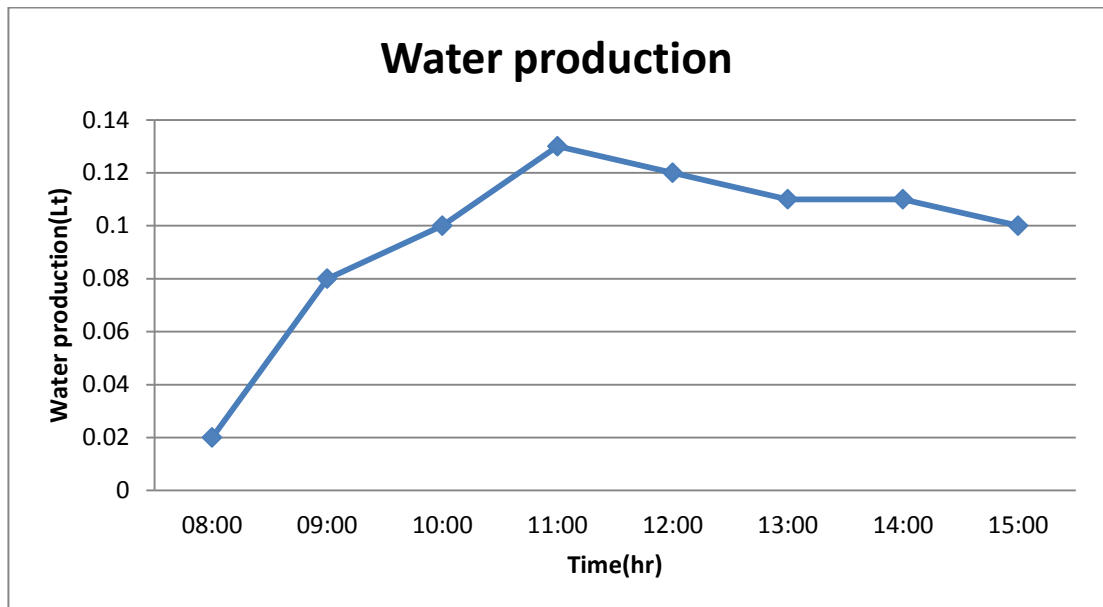


Figure 5-15: Hourly Water Production during the Day of January 5th

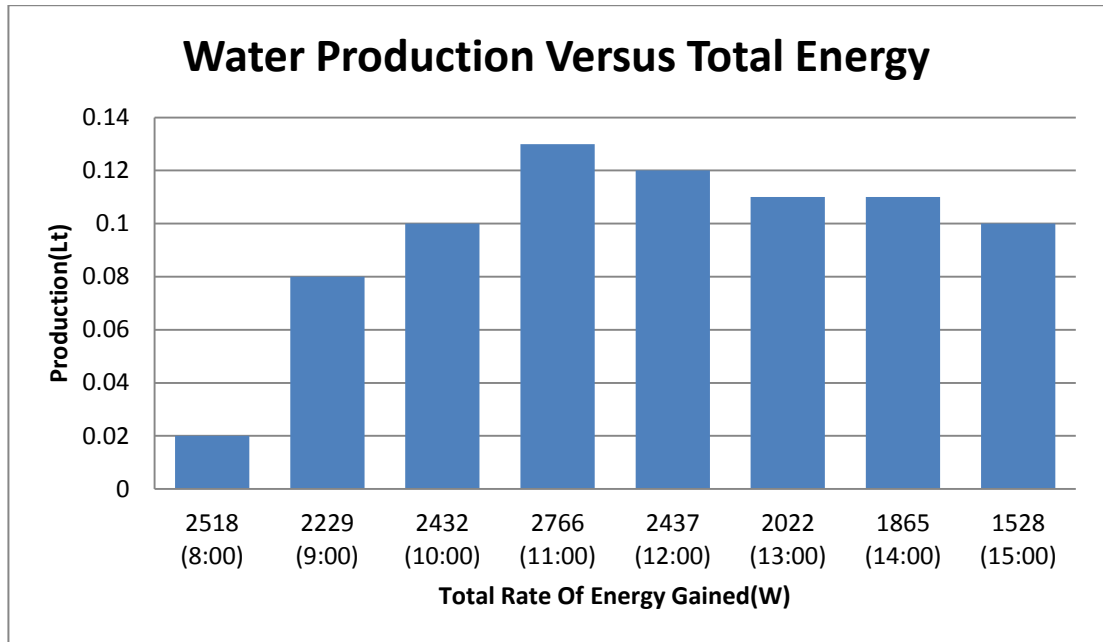


Figure 5-16: Water Production versus Total Rate of Energy Gained On January 5th,
(Total Energy = Solar Energy + Electrical Energy)

According to the psychrometric chart, the relative humidity of inlet air into the evaporator is 20%.

On January 6th the experiment is conducted by the water flow rate of 4 Lt/min and the air flow rate of 1.5 m³/min. whilst the water temperature is kept roughly 35°C.

The observed results of the experiment on January 6th are tabulated in Table 5.7.

Table 5-7: Observed Values of the Experiment on January 6th

t	Rad W/m ²	T _{amb} °C	H _{amb} %	T _{a,eva,in} °C	T _{a,eva,out} °C	T _{w,eva,out} °C	T _{a,cond,out} °C	T _{w,cond,in} °C	T _{w,cond,out} °C	T _{w,eva,in} °C	Pr Lit
8:00	514.5	9.8	91	24.5	14.1	18.5	10.5	7.1	8	33.1	0.09
9:00	766.5	13.1	81	37.9	27.6	31.2	14.3	10	15.9	34.3	0.16
10:00	840	15	66	48.4	29.2	32.7	15.2	12.9	16.9	35.3	0.26
11:00	1008	16	63.5	52.2	31.4	33.4	16	13.1	16.8	35.8	0.29
12:00	1039	16.8	58	60.2	31.7	34.2	17.1	13.2	17.2	35.6	0.3
13:00	924	16.7	52	54.1	30.3	33.6	16.9	12.8	16.9	35.4	0.28
14:00	168	15.6	61	34	29.8	32.9	16.6	11.2	16.7	35.9	0.26
15:00	420	16.2	63	33.4	28.9	30.1	16.5	10.3	16.5	34.8	0.27
ave	710	14.9	66.9	43.1	27.9	30.8	15.4	11.3	15.6	35	Tot= 1.91

As it illustrated in table 5.7, decreasing in the air flow rate, increases the temperature difference of the air in the condenser. Therefore, the water production is increased.

Diagram of changing the radiation during the day is illustrated in Figure 5.17, and the variation of water production is indicated in Figure 5.18. The variation of water production with the total rate of energy gained is presented in Figure 5.19.

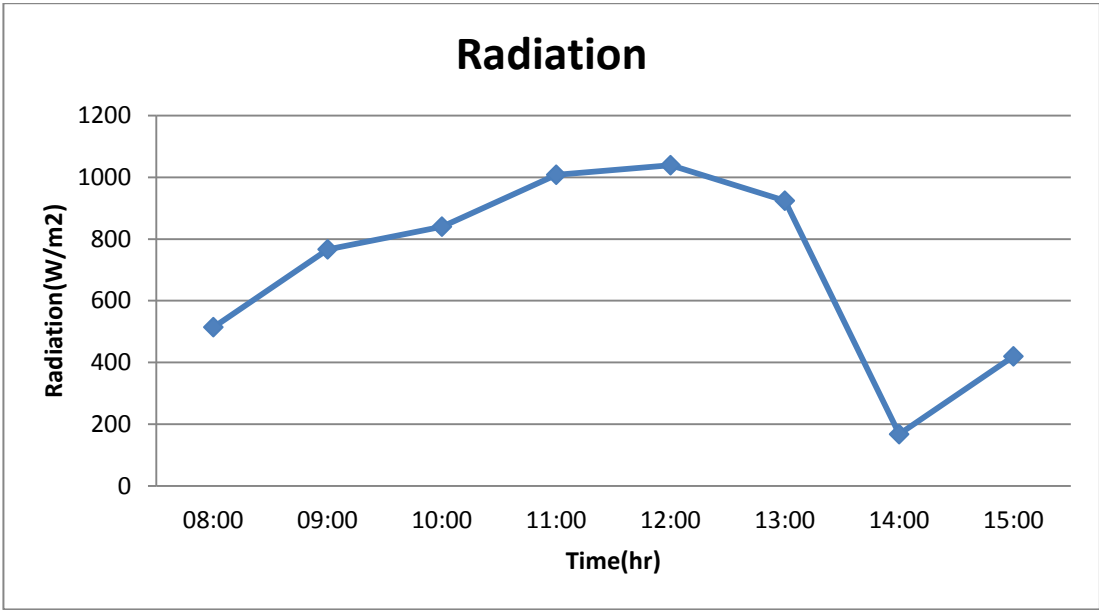


Figure 5-17: Variation of Irradiance during the January 6th

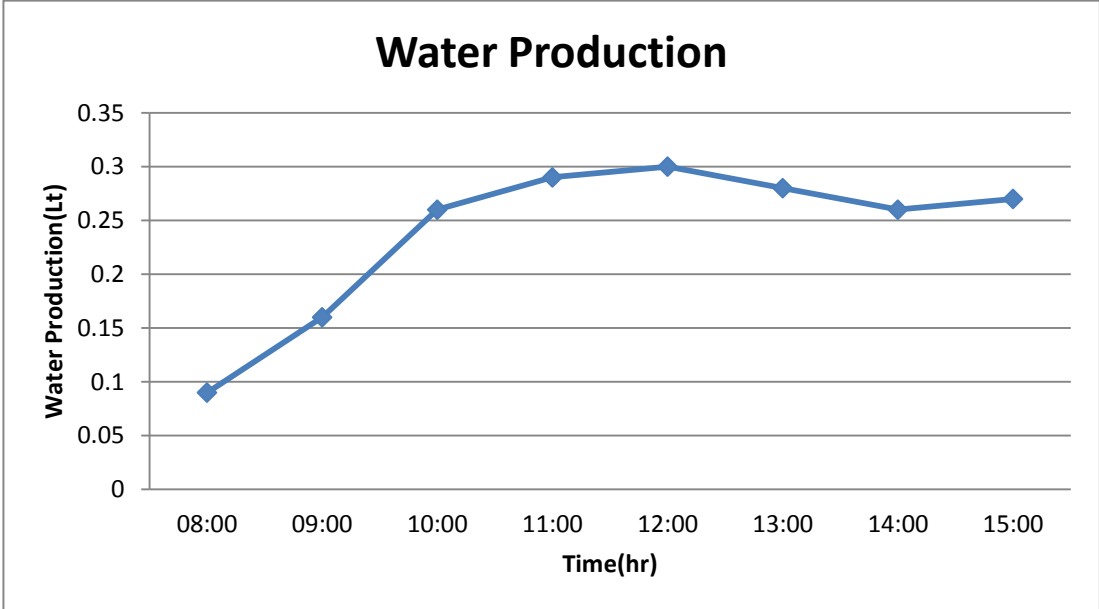


Figure 5-18: Hourly Production of Water during January 6th

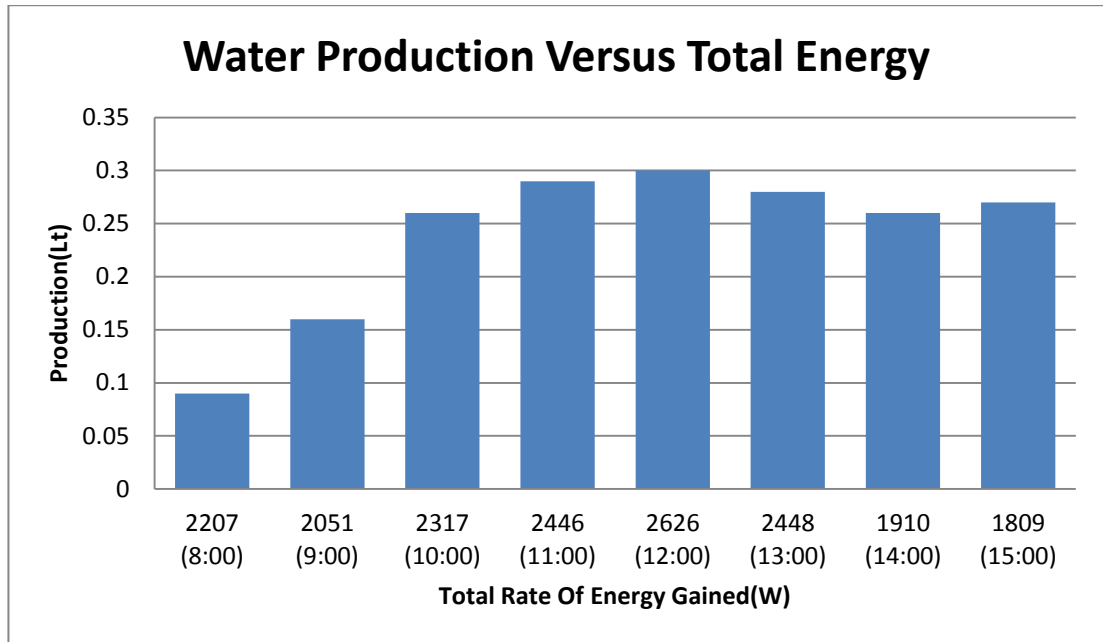


Figure 5-19: Water Production versus Total Rate of Energy Gained On January 6th,
(Total Energy = Solar Energy + Electrical Energy)

The relative humidity of the inlet dry air into the evaporator can be evaluated by using the psychometric chart; this reveals the relative humidity of 14% for the dry air.

On January 7th the experiment is conducted by adjusting the water flow rate of 6 Lt/min, whilst the air flow rate is 1.5 m³/min, and the inlet temperature of water kept around 35°C. The results of mentioned experiment are tabulated in Table 5.8.

Table 5-8: Observed Values of the January 7th

t	Rad W/m ²	T _{amb} °C	H _{amb} %	T _{a,eva,in} °C	T _{a,eva,out} °C	T _{w,eva,out} °C	T _{a,cond,out} °C	T _{w,cond,in} °C	T _{w,cond,out} °C	T _{w,eva,in} °C	Pr Lit
8:00	367.5	9.6	92	23.3	13.7	18.3	12.6	7.1	7.3	34.1	0.16
9:00	31.5	10.2	91	18.1	24.2	30.1	13.1	10	10.9	34.9	0.2
10:00	829.5	16.8	56	35.5	27.2	31.4	14.4	12.9	14.1	35.3	0.31
11:00	913.5	17.5	56	45.3	31.1	32.9	15.3	13.1	15	35.8	0.33
12:00	892.5	17.3	52	43.2	31.2	33.1	14.8	13.2	14.9	35.6	0.31
13:00	273	17	52	40.1	30.8	31.8	14.3	12.8	15.1	35.2	0.29
14:00	136.5	16.3	54	28.5	30.1	31.9	13.7	11.2	14.5	35.6	0.28
15:00	105	16	55	21.3	29.2	30.1	13.6	10.3	12.6	35.4	0.28
ave	444.7	15.1	63.5	31.9	27.3	30	14	11.3	13	35.2	Tot= 2.16

As it indicated in Table 5.8, the temperature of water in the condenser is slightly increased, but the air temperature drop is significant. It is because of high flow rate of water and low flow rate of air.

The hourly changes of radiation and water production through the day are shown in Figures 5.20 and 5.21, correspondingly. Besides, in Figure 5.22 the variation of water production proportional to the total rate of energy gained is illustrated.

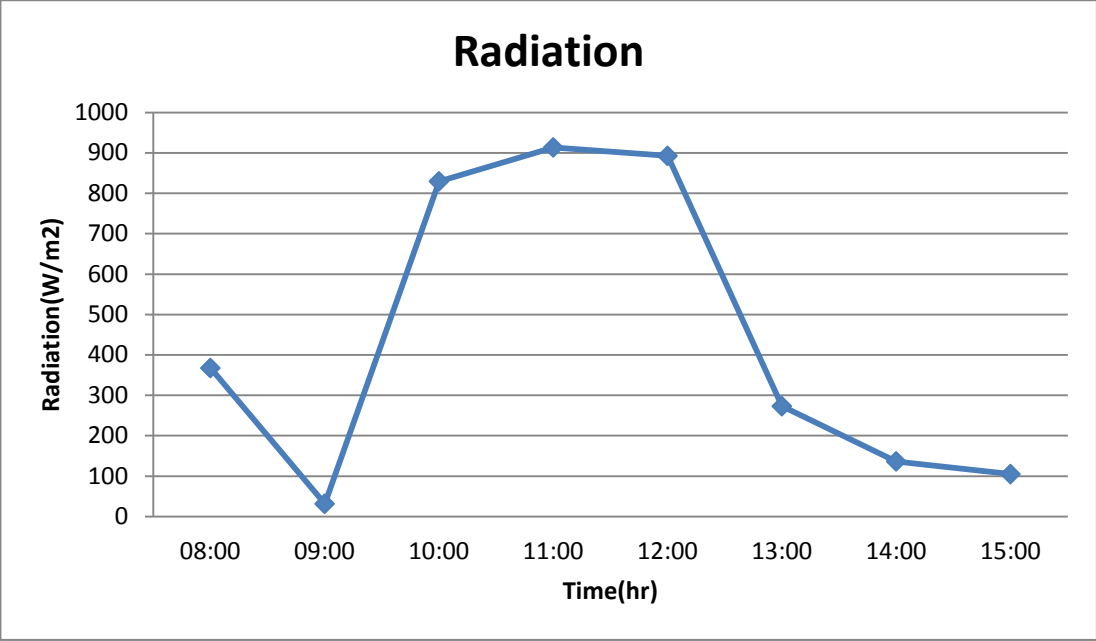


Figure 5-20: Variation of Insolation on January 7th

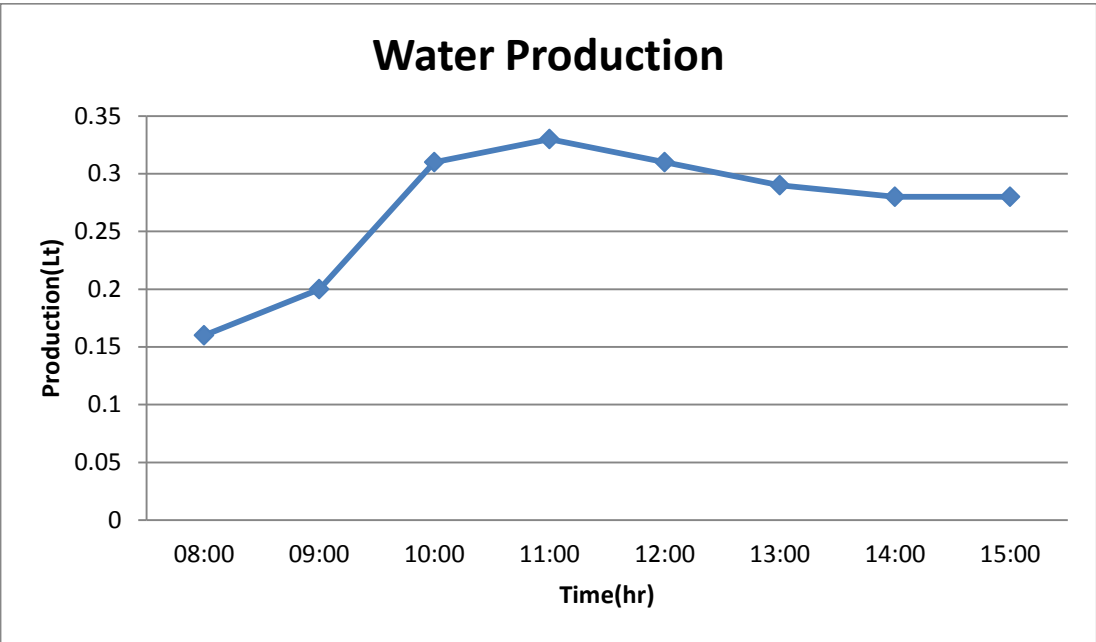


Figure 5-21: Hourly Changing the Water Production on January 7th

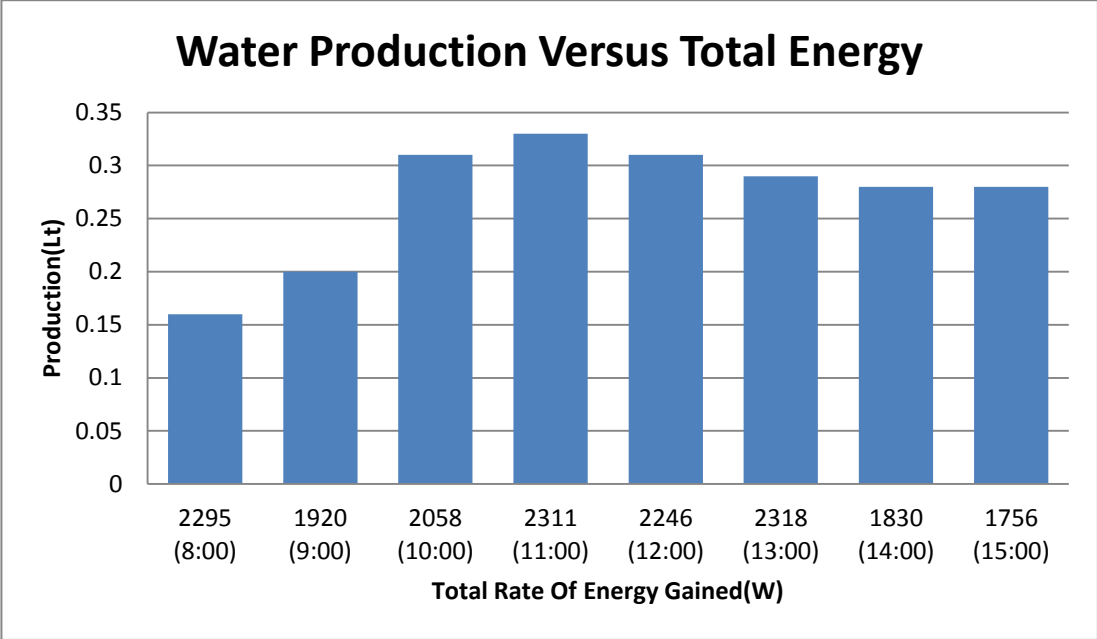


Figure 5-22: Water Production versus Total Rate of Energy Gained On January 7th,
(Total Energy = Solar Energy + Electrical Energy)

The relative humidity of the air at evaporator inlet, according to the psychometric chart is 30%.

The experiment on January 8th is conducted with the air flow rate of 1.5 m³/min; the water flow rate is adjusted on 6 Lt/min and the water temperature is adjusted on 55°C. Results of the experiment are tabulated in Table 5.9.

Table 5-9: The Measured Values on January 8th

t	Rad W/m ²	T _{amb} °C	H _{amb} %	T _{a,eva,in} °C	T _{a,eva,out} °C	T _{w,eva,out} °C	T _{a,cond,out} °C	T _{w,cond,in} °C	T _{w,cond,out} °C	T _{w,eva,in} °C	Pr Lit
8:00	178.5	11.9	91	18	16.1	33.3	13.3	7.4	7.6	53.2	0.16
9:00	168	12.5	85	17.4	27.8	34.1	13.9	8.6	10.2	55.6	0.31
10:00	84	10.4	94	20.4	30.4	37.2	15.6	8.7	9.6	55.9	0.36
11:00	220.5	13	79	29.7	34.3	39.1	15.8	10.8	12.1	55.8	0.43
12:00	84	12.8	85	24.7	33.1	39.6	15.5	11.1	12.3	55.6	0.4
13:00	1039	15.5	75	40.2	36.4	40.1	16.1	11.8	14.2	56.2	0.51
14:00	147	15.4	69	35.3	35.8	39.8	15.7	12	13.8	55.9	0.46
15:00	31.5	14.8	76	18.5	35	39.9	15.1	11.3	13.2	55.4	0.45
ave	244.1	13.3	81.7	25.5	31.1	37.9	15.1	10.2	11.6	55.4	Tot= 3.08

As the table implies the January 8th is a cloudy day with very low irradiance. The mean temperature difference of air in the condenser is measured to be 16°C, which is rather small. On the other hand, the amount of produced water is acceptable. This phenomenon is because of the low flow rate of air. Therefore, time of evaporation and condensation would be increase. Consequently, the efficiency of evaporator and condenser would be increase.

The variations of insolation and water production during the day are shown in Figure 5.23 and 5.24, respectively. Variation of water production with respect to the total rate of energy gained by the whole unit is graphed in Figure 5.25.

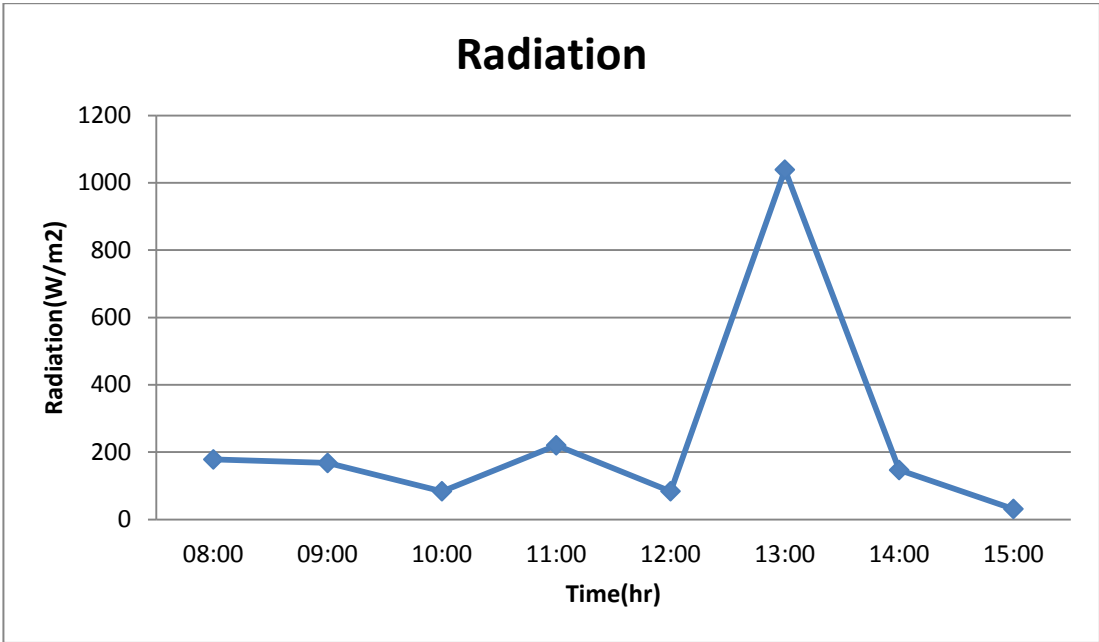


Figure 5-23: Hourly Changing Of Irradiance on January 8th

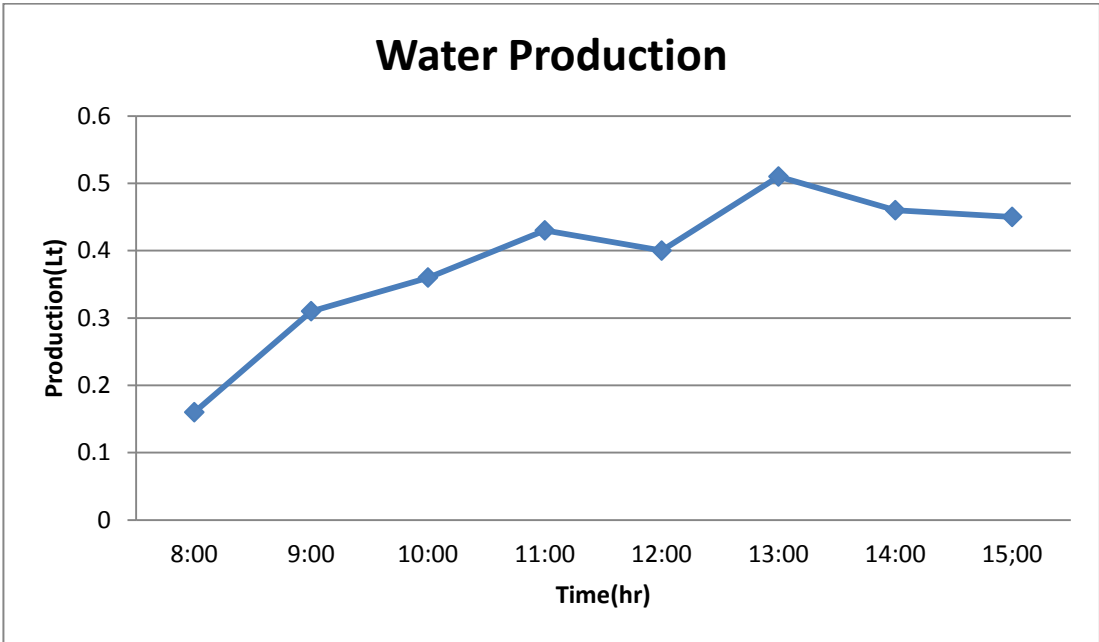


Figure 5-24: Hourly Changing Of Water Production during January 8th

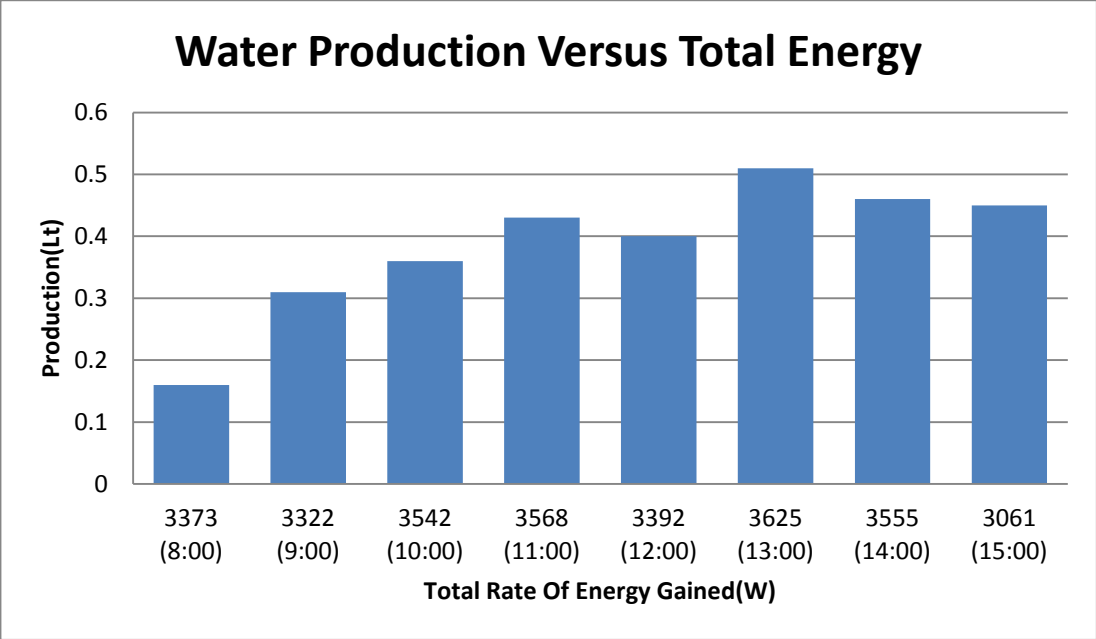


Figure 5-25: Water Production versus Total Rate of Energy Gained On January 8th,
(Total Energy = Solar Energy + Electrical Energy)

As it observed in this experiment, proportionality of the water and air flow rates can optimize the potable water production. Therefore, the potable water production may increase with readjusting the flow rates of water and air.

The water production in a humidification dehumidification desalination unit, which using air and water heaters mutually, mostly depends on the water temperature.

Chapter 6

CONCLUSIONS AND FUTURE WORK

6.1 Conclusions

The present work is concerned with the setting up and conduction of an experiment on a humidification-dehumidification desalination system that was designed by Kraft et al. [4]. The experiment is carried out under North Cyprus winter condition. A review of the previous studies and experiments is also made by providing brief description of their works. Additionally the governing equations, for each part of the unit are introduced and discussed. At the beginning of the study only air heating technique is employed, but the water production using only air heating method was almost zero. Therefore, water heating technique as well as air heating is applied. Finding the optimum flow rates for both water and the air was the intention of the experiment. The maximum production of potable water was achieved to be 3.1 Lt for the air flow rate of 1.5 m³/min, and water flow rate of 4 Lt/min for the condenser, and 1 Lt/min for the evaporator, whilst the water temperature was kept at 55°C. The hourly average rate of total energy gained by the whole unit is 3775 W. In the present work it is observed that with the lower flow rate of air, higher flow rate of water and higher evaporator inlet temperatures for both water and air, the productivity of potable water will increase.

6.2 Future Work

Justifying on the observations of the experiment would help us to find the solutions for the issues of the empiric. In this experiment, it is observed that the energy consumption is too much. Besides, the volume of humidifier is not proper for the absorption surface of the collector. Furthermore, the current unit must be leveled with high accuracy; otherwise, extraction of potable water from the dehumidifier would be impossible, or the saline water may be mix with the potable water. Moreover, the saline water is passing through the pipes; therefore, the scaling phenomenon will happen in time. Also, passing the cooling fluid inside the pipes may decrease the efficiency of the condenser. Likewise, the flow pattern in the humidifier is parallel, which is decreasing the efficiency of the evaporator. In addition, the air blower is sucking the air from the evaporator, which the fan may be damaged because of the high relative humidity of the air at that point. The following suggestion may help to solve the problems.

First of all a solar water collector has to be designed and installed instead of the electric water heater in order to decrease the energy consumption of the system. The humidifier must be replaced with a smaller evaporator, and the flow pattern must be change to counter current in order to maximize the evaporation. A slight slope needs to be considered for the condenser in order to help the water extraction. Additionally, to prevent the scaling phenomenon inside the tubes of condenser, saline water should be pass through the shell side of the condenser, which it may increase the efficiency of the dehumidifier as well. Finally, it is better to position the fan at the entrance of solar air collector in order to prevent corrosion of the fan.

REFERENCES

- [1] Kalogirou S.A, "Survey of solar desalination systems and system selection," *energy*, vol. 22, pp. 69-81, 1997.
- [2] Ettouney Hisham, Fawzy, Nagla Al-Enzi Ghazi, "low temperature humidification dehumidification desalination process," *Energy Conversion And Management*, vol. 47, pp. 470-484, 2006.
- [3] Forbes S, Feeley T Hoffmann.J, *Estimating freshwater needs to meet 2025 electricity generating capacity forecasts.:* US Department of Energy/National Energy Technology Laboratory, 2004.
- [4] Kraft R, Atikol U "pilot project SOLARDES Y- solar desalination system with cascading evaporation in northern Cyprus," in *10th International Conference on Clean Energy(ICCE 2010)*, famagusta, 2010.
- [5] Sharqawy Mostafa H, Summers Edward K, Lienhard John H, Zubair Syed M, Antar M.A, Prakash Narayan G, "The potential of solar driven humidification dehumidification desalination for small scale decentralized water production," *Renewable And Sustainable Energy Reviews*, vol. 14, pp. 1187-1201, 2010.
- [6] Nirmalakhandan Nagamany, Deng Shuguang Gnaneswar, Gude Veera, "desalination using solar energy," *Towards sustainability*, 2010.
- [7] Kotb H, Mostafa G.H, Ghalban A.R, Amer E.H, "Theoretical and Experimental Investigation of Humidification-Dehumidification Desalination Unit," *Desalination*, vol. 249, pp. 949-959, 2009.

- [8] Galanis N, Laplante M, Orfi J, "Air humidification dehumidification for water desalination system using solar energy," *DESALINATION*, vol. 203, pp. 471-781, 2006.
- [9] Mitsos Alexander, Lienhard V, John H Mistry, Karan H, "Optimal operating condition and configurations for humidification dehumidification desalination cycles," *International Journal Of Thermal Sciences*, vol. 50, pp. 779-789, 2011.
- [10] Amidpour M, Mehrgoo M, "Constructal design of humidification dehumidification desalination unit architecture," *Desalination*, vol. 271, pp. 62-71, 2011.
- [11] Parkesh Sandeep, Selman J.R, AL-Hallaj Said, Farid M.M, "Solar desalination with a humidification dehumidification cycle: mathematical modeling of the unit," *Desalination*, vol. 151, pp. 153-164, 2002.
- [12] Behzadmehr A, Farsad S, "Analysis of a solar desalination unit with humidification dehumidification cycle using DoE method," *Desalination*, 2011.
- [13] Zamen M, Amidpour M, Soufari S.M, "performance optimization of the humidification dehumidification desalination process using mathematical programming," *Desalination*, vol. 237, pp. 305-317, 2009.
- [14] Parekh Sandeep, Farid M.M, Selman J.R, Al-Hallaj Said, "Solar desalination with humidification dehumidification cycle: review of economics," *Desalination*, vol. 195, pp. 169-186, 2006.
- [15] Hsieh H.S, *solar engineering*. New jersey, 1991.
- [16] Boles Michael.A cengel, Yunus A, *Thermodynamics an engineering approach* , fifth edition ed.
- [17] Treybal Robert.E, *Mass transfer operation*, third edition ed. Rhole Island:

McGraw-Hill book company, 1981.

[18] Holman J.P, *Heat transfer*, sixth edition ed.: McGraw-Hill book company,
1986.

APPENDIX

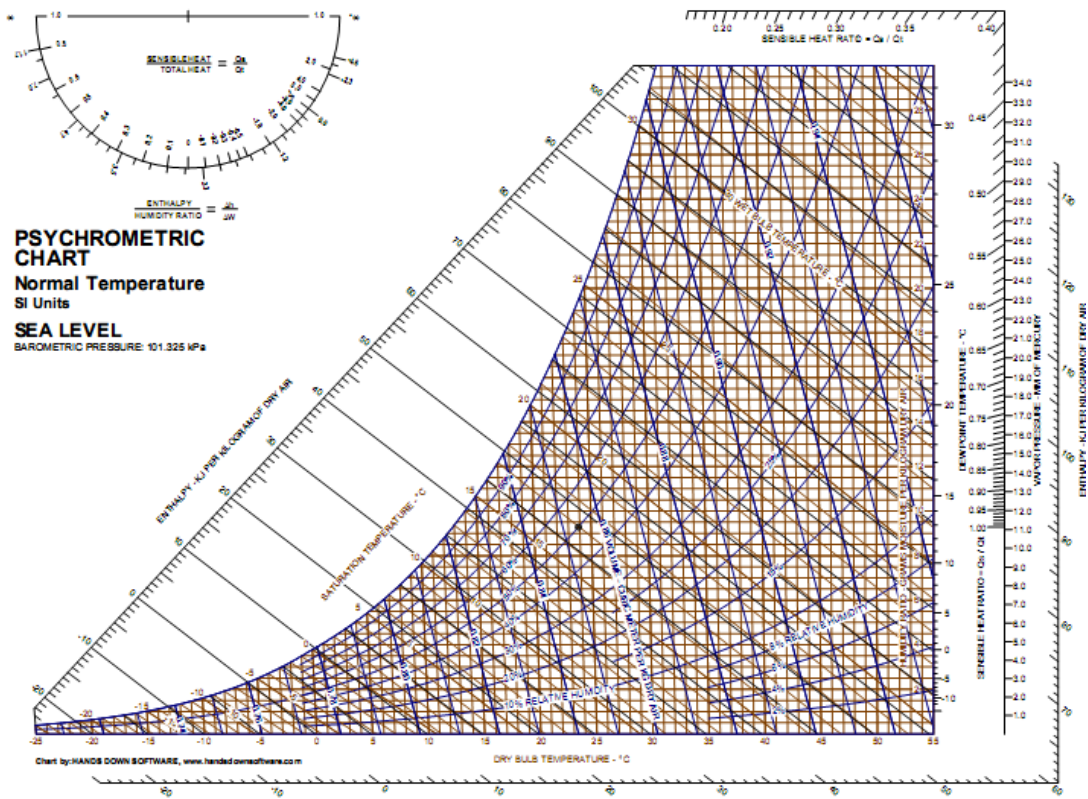


Figure A-1: psychrometric chart